

การโน้ตเรดชันของอคูมิเนียมอัลลอยด์และเหล็ก H13 โดยพลามาจากการควบคุมแปลง
เหนี่ยวนำคลื่น



นางสาว จิราภรณ์ พงษ์โสภา

ศูนย์วิทยทรัพยากร จุฬาลงกรณ์มหาวิทยาลัย

วิทยานิพนธ์นี้เป็นส่วนหนึ่งของการศึกษาตามหลักสูตรปริญญาวิทยาศาสตรดุษฎีบัณฑิต

สาขาวิชาวิทยาศาสตร์นาโนและเทคโนโลยี (สหสาขาวิชา)

บัณฑิตวิทยาลัย จุฬาลงกรณ์มหาวิทยาลัย

ปีการศึกษา 2553

ลิขสิทธิ์ของจุฬาลงกรณ์มหาวิทยาลัย

NITRIDATION OF ALUMINIUM ALLOYS AND AISI H13 TOOL STEEL BY INDUCTIVE
COUPLED RF PLASMA



Miss Jiraporn Pongsopa

ศูนย์วิทยทรัพยากร

จุฬาลงกรณ์มหาวิทยาลัย
A Dissertation Submitted in Partial Fulfillment of the Requirements
for the Degree of Doctor of Philosophy Program in Nanoscience and Technology

(Interdisciplinary Program)

Graduate School

Chulalongkorn University

Academic Year 2010

Copyright of Chulalongkorn University

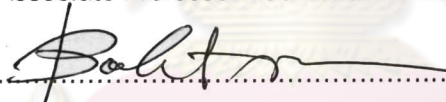
Thesis Title NITRIDATION OF ALUMINIUM ALLOYS AND AISI H13 TOOL
STEEL BY INDUCTIVE COUPLED RF PLASMA
By Miss Jiraporn Pongsopa
Field of Study Nanoscience and Technology
Thesis Advisor Assistant Professor Boonchoat Paosawatyanong, Ph.D.
Thesis Co-advisor Assistant Professor Patama Visuttiptukul, Ph.D.


Accepted by the Graduate School, Chulalongkorn University in Partial Fulfillment
of the Requirements for the Doctoral Degree



..... Dean of the Graduate School
(Associate Professor Pornpote Piumsomboon, Ph.D.)


THESIS COMMITTEE



..... Chairman
(Associate Professor Vudhichai Parasuk, Ph.D.)


..... Thesis Advisor
(Assistant Professor Boonchoat Paosawatyanong, Ph.D.)


..... Thesis Co-advisor
(Assistant Professor Patama Visuttiptukul, Ph.D.)


..... Examiner
(Assistant Professor Sukkaneste Tungasmita, Ph.D.)


..... Examiner
(Stephan Dubas, Ph.D.)


..... External Examiner
(Associate Professor Surasing Chaiyakun, Ph.D.)

จิราภรณ์ พงษ์โสภา : การไนไตรเดชันของอลูมิเนียมอัลลอยด์และเหล็กกล้า H13 โดยพลาสมาจากการควบคุมแปลงเหนี่ยวนำคลื่น. (NITRIDATION OF ALUMINIUM ALLOYS AND AISI H13 BY INDUCTIVE COUPLED RF PLASMA) อ. ที่ปรึกษาวิทยานิพนธ์หลัก: ผศ.ดร.บุญโชติ เผ่าสวัสดิ์ขจรยง, อ. ที่ปรึกษาวิทยานิพนธ์ร่วม: ผศ.ดร.ปรุมา วิสุทธิพิทักษ์กุล, 99 หน้า.

การวิจัยนี้เป็นงานวิจัยที่เกี่ยวข้องกับ การพัฒนาสมบัติของพื้นผิว โดยการผลิตชั้นไนไตรด์บนอลูมิเนียมอัลลอยด์ 2011 และเหล็กกล้าเครื่องมือ H13 ด้วยการไนไตรเดชันโดยใช้ระบบพลาสมาแบบคลื่นความถี่วิทยุจากการควบคุมแปลงเหนี่ยวนำคลื่น ซึ่งจุดประสงค์หลักของงานวิจัยนี้คือการเกิดชั้นไนไตรด์บนผิวของอลูมิเนียมอัลลอยด์ 2011 และเหล็กกล้าเครื่องมือ H13 โดยการไนไตรเดชันด้วยพลาสมาจากการควบคุมแปลงเหนี่ยวนำคลื่น ที่อุณหภูมิต่ำกว่า 350°C ภายใต้สภาวะพลาสมาที่กำลังไฟฟ้า ความดัน อุณหภูมิ และเวลาที่แตกต่างกัน ซึ่งจากการทดลองพบว่ามีเกิดการเกิดชั้นอลูมิเนียมไนไตรด์ (AlN) บนชิ้นงานอลูมิเนียมอัลลอยด์ 2011 และ เหล็กไนไตรด์ (FeN) บนชิ้นงานเหล็กกล้าเครื่องมือ H13 โดยการวิเคราะห์ด้วยเทคนิคเอกซเรย์ดิฟแฟรกชัน สำหรับการไนไตรเดชันบนอลูมิเนียมอัลลอยด์ 2011 เกิดชั้นไนไตรด์ที่บางมากและมีความหนาสูง ทำให้ไม่สามารถวัดความหนาและความแข็งของชิ้นงานได้ ในขณะที่ชิ้นงานเหล็กกล้าเครื่องมือ H13 ที่ผ่านกระบวนการเดียวกันสามารถเกิดชั้นไนไตรด์ที่มีความหนามากกว่า $150\ \mu\text{m}$ และ มีความแข็งเพิ่มขึ้น 1072 HV ที่ระยะเวลาไนไตรเดชัน 20 ชั่วโมง

ศูนย์วิทยทรัพยากร
จุฬาลงกรณ์มหาวิทยาลัย

สาขาวิชา วิทยาศาสตร์นาโนและเทคโนโลยี ลายมือชื่อนิติศ.....

ปีการศึกษา 2553

ลายมือชื่อ อ.ที่ปรึกษาวิทยานิพนธ์หลัก 

ลายมือชื่อ อ.ที่ปรึกษาวิทยานิพนธ์ร่วม 

##4989717020 : MAJOR NANOSCIENCE AND TECHNOLOGY

KEYWORDS : PLASMA NITRIDING/RF-ICP/ ALUMINIUM ALLOY/AISI H13

JIRAPORN PONGSOPA: NITRIDATION OF ALUMINIUM ALLOYS AND AISI H13
TOOL STEEL BY INDUCTIVE COUPLED RF PLASMA. ADVISOR: ASST. PROF.
BOONCHOAT PAOSAWATYANYONG, Ph.D., CO-ADVISOR: ASST. PROF.
PATTAMA VISUTTIPITUKUL, Ph. D., 99 pp.

RF-ICP plasma nitriding is used to improve surface property by producing a nitride layer on the specimen. The main aim of this work is to form the nitride layer on the surface of Al alloy and AISI H13 by RF-ICP plasma nitriding with the treatment temperature lower than 350 °C. The specimens were plasma nitrided at different treatment times while the rf-power, working pressure and treatment temperature were kept constant. After plasma nitriding, the nitride layers including AlN, FeN were present in the aluminium alloy sample and H13 sample, respectively, as detected by X-ray diffraction analysis. In the case of the Al alloy, the hardness of the nitrided sample is difficult to measure because of the thin layer of nitride on the sample surface and high roughness. Moreover, the thick AlN did not form when we varied the parameters including the type of gas sputtering, treatment time, and gas pressure. Therefore, we can conclude that rf plasma nitriding is not suitable for aluminium alloys. On the contrary, in the rf plasma nitriding of H13, the thickness of the nitride layer reaching more than 150 µm was achieved for 20 hours with the hardness as high as 1072 HV.

Field of Study : Nanoscience and Technology

Academic Year..... 2010

Student's Signature _____

Advisor's Signature _____

Co-advisor's Signature _____

ACKNOWLEDGEMENTS

I am deeply grateful to my advisor, Asst. Prof. Dr. Boonchoat Paosawatyanong, and my co-advisor, Asst. Prof. Dr. Patama Visuttipitukul, for suggestion, perspective, constructive comments, and important support throughout this work.

I would like also thank Assoc. Prof. Dr. Vudhichai Parasuk, Director of Nanoscience and Technology Program, who gave me a kind suggestion and Asst. Prof. Dr. Sukkaneste Tungasmita, Deputy director of Nanoscience and technology Program, Dr. Ratthapol Rangukupan, Secretary of Nanoscience and Technology program, whose advised me with important guidance during my Ph.D. studies.

My warm thanks go to Prof. Pichet Limsuwan and Asst. Prof. Dr. Sukkaneste Tungasmita, who help me with nanoindentation measuring, and Assoc. Prof. Dr. Surasing Chaiyakun, for interesting discussions on the vacuum system. I wish to thank Dr.dusit Ngamrungrroj and Dr.Kanchaya Honglertkongsakul, for their help in plasma experiments.

I owe my loving thanks to my dad and mum. Without their encouragement and understanding it would have been impossible for me to finish my work.

The financial support provide to me by Graduate School and Nanoscience and Technology Program, Chulalongkorn University, for the travel grant to conference abroad.

I would like to acknowledge the postgraduate scholarship provided by Suan Dusit Rajabhat University.

Lastly, a big 'thank you' to nanoscience friends, for lovely comfort, my colleagues in plasma lab, for make me smile during I got bad situation. My thanks extend to all who have in anyway helped me but I might have not mentioned here.

CONTENTS

| | Page |
|---|----------|
| ABSTRACT (THAI)..... | iv |
| ABSTRACT (ENGLISH)..... | v |
| ACKNOWLEDGEMENTS..... | vi |
| CONTENTS..... | vii |
| LIST OF TABLES..... | x |
| LIST OF FIGURES..... | xi |
| CHAPTER I INTRODUCTION..... | 1 |
| 1.1 Thesis motivation..... | 1 |
| 1.2 Purpose of this work..... | 3 |
| 1.3 Scope and thesis organization..... | 3 |
| CHAPTER II REVIEW OF LITERATURE AND THEORETICAL BACKGROUND.... | |
| 2.1 Chapter review..... | 5 |
| 2.2 Aluminium and aluminium alloys..... | 5 |
| 2.3 Hot work tool steel..... | 6 |
| 2.4 The nitride of metals..... | 7 |
| 2.5 Techniques for the formation of nitride layer..... | 8 |
| 2.5.1 Physical vapor deposition..... | 9 |
| 2.5.2 Chemical vapour deposition..... | 10 |
| 2.5.3 Plasma immersion ion implantation..... | 10 |
| 2.5.4 Traditional nitriding methods..... | 13 |
| 2.5.5 Plasma nitriding process..... | 11 |
| 2.6 Emission spectroscopy of gas discharge..... | 17 |
| 2.7 Power source to plasma nitriding techniques..... | 18 |
| 2.7.1 DC plasma nitriding..... | 18 |
| 2.7.2 rf plasma nitriding..... | 19 |

| | |
|--|----|
| 2.8 Influence of processing parameters on plasma nitriding | |
| 2.8.1 Addition hydrogen in plasma nitriding..... | 24 |
| 2.8.2 Effect of plasma treatment time..... | 25 |
| 2.8.3 Effect of heat temperature..... | 25 |
| CHAPTER III EXPERIMENT TECHNIQUES..... | |
| 3.1 The material investigated..... | 27 |
| 3.2 Substrate preparation..... | 27 |
| 3.3 Nitriding equipment..... | 28 |
| 3.4 Nitriding procedure..... | 30 |
| 3.5 Nitriding cobditions..... | 30 |
| 3.6 Characterization techniques..... | 31 |
| 3.7 Morphology and composition..... | |
| 3.7.1 X-Ray diffraction analysis..... | 31 |
| 3.7.2 Scanning electron microscopy..... | 34 |
| 3.7.3 Electron probe micro analyzer..... | 35 |
| 3.7.4 Atomic force microscopy..... | 36 |
| 3.7.5 Optical microscopy..... | 37 |
| 3.7 Plasma diagnostic..... | 38 |
| 3.8 Techniques for mechanical properties..... | |
| 3.8.1 Vicker hardness test..... | 39 |
| 3.8.2 Nanoindentation..... | 39 |
| CHAPTER IV CHARACTERSATION OF THE NITRIDED LAYERS OF | |
| ALUMINIUM ALLOY..... | |
| 4.1 Chapter review..... | 41 |
| 4.2 Material investigated..... | 42 |
| 4.3 Influence of rf plasma nitriding edge effect of aluminium alloy..... | 42 |
| 4.4 Effect of sputtering in plasma nitriding of aluminium alloy..... | 44 |
| 4.5 Effect of treatment time..... | |

| | |
|---|----|
| 4.5.1 Experiment, results and discussions..... | 46 |
| 4.5.2 Summary..... | 51 |
| 4.6 The effect of hydrogen in rf plasma nitrided aluminium alloy..... | |
| 4.6.1 Experiment, results and discussions..... | 51 |
| 4.7 Effect of rf power..... | 61 |
| 4.7.1 Summary..... | 61 |
| | |
| CHAPTER V CHARACTERIZATION OF THE NITRIDED LAYERS OF AISI H13 STEEL..... | |
| 5.1 Chapter review..... | 62 |
| 5.2 Effect of sample..... | 63 |
| 5.3 Effect of treatment time..... | |
| 5.3.1 Experiment, results and discussions..... | 64 |
| 5.3.2 Summary..... | 81 |
| CHAPTER VI CONCLUSIONS..... | 82 |
| REFERENCES..... | 84 |
| APPENDICES..... | 95 |
| VITAE..... | 99 |

ศูนย์วิทยทรัพยากร
จุฬาลงกรณ์มหาวิทยาลัย

LIST OF TABLES

| Table | Page |
|---|------|
| 2.1 Physical properties of Al and AlN..... | 7 |
| 2.2 Summary of experimental conditions for DC plasma nitriding from published literature..... | 19 |
| 2.3 Comparison of plasma parameters in different power source using Langmuir probe..... | 23 |
| 2.4 Summary of experimental conditions for DC plasma nitriding from published literature..... | 23 |
| 2.5 Surface temperature (Tk) for different quantitative of H ₂ | 25 |
| 2.6 Diffusion coefficient of nitrogen and chromium at several temperatures..... | 26 |
| 3.1 The chemical composition of Al 2011 and AISI H13 (wt%)..... | 27 |
| 4.1 Conditions of nitriding on Al 2011..... | 40 |
| 5.1 Surface hardness of nitride sample..... | 78 |
| 6.2 Er ,H and Wtotal of nitrided sample..... | 79 |

ศูนย์วิทยทรัพยากร
 จุฬาลงกรณ์มหาวิทยาลัย

LIST OF FIGURES

| Figure | | Page |
|--------|---|------|
| 2.1 | Diagram of engineering methods for surface hardening of steels.. | 9 |
| 2.2 | Model of iron nitriding in DC plasma nitriding..... | 16 |
| 2.3 | Phenomena influencing the atomic nitrogen concentration at the surface of an iron or steel sample during plasma nitriding..... | 17 |
| 2.4 | Graph of ion striking decrease and the flux of neutral radicals increase with pressure..... | 21 |
| 2.5 | (a) Typically CCP discharge, (b) ICP discharge with helix, and (c) ICP discharge with planar antenna..... | 21 |
| 3.1 | The plasma nitriding system as installed at plasma laboratory..... | 29 |
| 3.2 | Diagram of x-ray diffraction..... | 32 |
| 3.3 | A Geometry of the Bragg-Brentano method..... | 33 |
| 3.4 | Geometry of the GIXRD method..... | 33 |
| 3.5 | Schematic representation electron signals from the specimen..... | 34 |
| 3.6 | Spectroscopy by WDS..... | 36 |
| 3.7 | The diagram of light in DF (a), and BF(b) mode..... | 38 |
| 4.1 | Surface morphology of a) Untreated sample, b) After pre-sputtering with Ar-H ₂ for 1 h, and c) After nitriding with N ₂ -H ₂ for 25 h..... | 43 |
| 4.2 | The atomic% of element including N, Al, Si and Cu at three zones (edge, interface and center) of nitrided sample for 25 h..... | 43 |
| 4.3 | 3D AFM images of nitride sample sputtered with different gas as (a) untreated, (b) Ar sputtering, and (c) Ar-H ₂ sputtering samples | 45 |
| 4.4 | Emission spectra of Ar and Ar-H ₂ mixture at 1 torr in wavelength of 450 nm to 900 nm..... | |

| Figure | Page |
|---|------|
| 4.5 SEM image of samples treated with nitriding process for (a) 9 hr, (b) 16 hr and (c) 25 hr..... | 47 |
| 4.6 Nitrogen and aluminium maps showing the distribution of nitrided surface at different nitriding time (a) 9 h; and (b) 16 h. The colored scale bar show the comparative concentration condition at 10 μm step size..... | 48 |
| 4.7 EDX analysis of nitrided Al2011 for 25 h..... | 48 |
| 4.8 GIXD pattern of nitride Al 2011 at 250 V bias voltages, 400°C treatment temperature..... | 50 |
| 4.9 EPMA/BSE micrograph of Al-6wt%Cu after plasma nitriding in 25% H_2 of total gas pressure..... | 54 |
| 4.10 EPMA/BSE micrograph of Al-6wt%Cu after plasma nitriding in 50% H_2 of total gas pressure..... | 54 |
| 4.11 EPMA/BSE micrograph of Al-6wt%Cu after plasma nitriding in 75% H_2 of total gas pressure..... | 55 |
| 4.12 EPMA/BSE micrograph of Al-6wt%Cu after plasma nitriding in pure nitrogen of total gas pressure..... | 55 |
| 4.13 SEM micrograph of Al-6wt%Cu after plasma nitriding in different gas mixture; (a) 25% H_2 ; (b) 50 % H_2 ; (c) 75 % H_2 (d) Pure Nitrogen..... | 56 |
| 4.14 The EPMA mapping of plasma nitrifying, pure nitrogen, at 250 W | 57 |
| 4.15 X-ray diffraction pattern of Al-6wt%Cu rf plasma nitriding at 200 W for 6 h, as various hydrogen percentages (a) 25% H_2 , (b) 50% H_2 , (c) 75% H_2 and (d) pure N_2 | 59 |
| 4.16 Emission spectra of N_2 - H_2 mixture at 0.5 torr in wavelength of 300 nm – 800 nm..... | 60 |
| 4.17 Al-6wt%Cu plasma nitriding with pure nitrogen at different rf power (a) 200 W (b) 250W..... | 61 |
| 5.1 The comparison of surface color after nitriding of: (a) 1h, (b) 9 h, | 63 |

| Figure | | Page |
|--------|---|------|
| | (c) 12 h. | |
| 5.2 | Appearance of AISI H13 samples (a) untreated, and (b) treated. | 65 |
| 5.3 | SEM micrographs of a AISI H13 surface treated at different time; (a)4 h, (b) 9h, (c)12 h, and (d) 20h..... | 66 |
| 5.4 | AFM images with nitriding time of: (a) untreated, (b) 9 h, (c) 12 h | 68 |
| 5.5 | The mount sample (12 h nitriding) for cross sectional testing..... | 63 |
| 5.6 | SEM cross section of AISI H13 nitriding for 20 h..... | 68 |
| 5.7 | Cross-sectional H13 sample treated for 9 h (a), and 20 h (b) at 300 °C..... | 69 |
| 5.8 | SEM micrograph showing the cross-section of edge of AISI H13 sample treated for 20 h..... | 70 |
| 5.9 | EDX composition profile of AISI H13 sample treated for 20 h..... | 71 |
| 5.10 | Electron probe microanalysis (EPMA) element maps (Fe, and N) of surface of the H13 treated at 20 h..... | 72 |
| 5.11 | Electron probe microanalysis (EPMA) element maps (Fe, N, and Cr) of cross-sectional of the H13 treated at 20 h..... | 72 |
| 5.12 | (a) Backscattered electron images showing the cross-section of nitrided H13 and (b) profiles of nitrogen, chromium, and iron concentration determined in the cross-section of nitrided H13 for 20 h..... | 73 |
| 5.13 | Coloring of nitride sample (a) and compositional line scan of the h13 if nitriding for 20 h; (b) nitrogen, (c) Iron; (d) Chromium..... | 74 |
| 5.14 | GIXD profiles at the incident angle of 3 degree of H13 sample after different nitriding time (1 to 20 hours)..... | 76 |
| 5.15 | The FWHM of the XRD peak and the corresponding grain size of the broadening peak at $2\theta=44^\circ$ as a function of the treatment time (1, 4, 9, 12, and 20 h)..... | 77 |
| 5.16 | Variation of surface hardness with nitriding time..... | 78 |

| Figure | | Page |
|--------|--|------|
| 5.17 | Element map showing the distribution of N, Si, Fe, Cr, O, V, and Al in a sample for treatment time 20 h..... | 80 |
| 5.18 | SEM micrograph of cross-section film deposited on silicon wafer during plasma nitriding AISI H13 for 20 h..... | 81 |



ศูนย์วิทยทรัพยากร
จุฬาลงกรณ์มหาวิทยาลัย

CHAPTER I

INTRODUCTION

1.1 Thesis motivation

Aluminium alloys and the hot working steels H13 are employed in different areas of contemporary industrial fabrication because of low specific weight [1] and good tempering resistance [2]. However, both materials have low wear resistance [3-4], and surface hardness. As we know, the surface engineering such as surface treatment, coating, and surface modification are used to increase surface hardness, minimize adhesion (reduce friction) and improve wear resistance for tool steel substrates [5]. Due to its high hardness, reports showed that the formation of the nitride layer remarkably increases the wear resistance of underlying alloys and steels [3]. Recently, there have been several kinds of techniques devised to form the nitride layers for automotive parts, e.g. ion-implantation, and plasma nitriding. The disadvantages of ion-implantation are difficult for scaling up to commercial size due to the high costs of manufacturing, and complications of equipment [6]. Therefore, over the last few decades, nitriding treatment has been studied in attempts to improve the tribological properties of ferrous alloy and non-ferrous alloy either by surface hardening or surface modification. In addition, various nitriding methods, e.g., gas nitriding, liquid nitriding, plasma nitriding are also called nitriding treatments in which nitrogen can penetrate into the substrate to form a nitride layer. Plasma nitriding, also called ion-nitriding or glow discharge nitriding has been preferred recently to most surface hardening applications because of their faster nitrogen penetration, cleanliness, and economical aspects [7-8]. Generally, DC plasma source was used to generate plasma for the plasma nitriding process, particularly in aluminium plasma nitriding, because of the uncomplicated source when compared with other plasma sources. However, DC plasma

nitriding used at high pressure (>1 torr) because it can be generated high plasma density, which can enhance the nitride layer. Moreover, they require high nitrogen gas pressure. Recently, rf plasma source is more frequently used in plasma nitriding because it can be operated at lower gas pressures [9] which are necessary to prevent continuous formation of the oxide layer during the nitriding process [10]. Moreover, other advantages include high plasma density, and high uniformity [11].

In the plasma nitriding of aluminium substrate, the nitrided surface can raise the hardness level because the nitrogen ions generated in plasma will diffuse into the aluminium matrix and form a aluminium nitride (AlN) layer. AlN has been known to have good dielectric properties, high hardness, high electrical resistivity, high thermal conductivity, high corrosion, and wear resistance and hence has been widely used in many applications [12-13]. For the successful plasma nitriding of aluminium alloys, the process should be performed using the two sub-processes of pre-sputtering and the nitriding process. Removal of surface aluminium oxide is a significant step to achieving an AlN layer mainly because naturally-formed aluminium oxide (Al_2O_3) prevents the nitrogen atom from diffusing into the aluminium alloy substrate [14]. The removal of Al_2O_3 from the Al surface is achieved by sputtering with inert gas or combined with non-inert gas [15], including argon, argon-nitrogen, argon-hydrogen, and so on. As for the nitriding process, the type of gas, substrate bias voltage, rf power and treatment temperature are important parameters for the successful formation of AlN on samples. However, high substrate bias voltage can cause severe surface roughening [13, 16-17].

In the plasma nitriding of AISI H13, the interaction of the nitrogen and steel components leads to the formation of different types of metallic nitride. Usually, the nitrided layer comprises a compound zone consisting of iron nitrides of ϵ phase ($\epsilon\text{-Fe}_{2-3}\text{N}$), gamma phase ($\gamma\text{-Fe}_4\text{N}$) or a mixed phase ($\epsilon + \gamma$) developed at the surface [1], and diffusion zone which beneath the compound layer consists mainly of interstitial N atoms in the solid solution [18] which is reached

as the nitride precipitates. However, the resulting structure of these domains depends on the time, substrate temperature, and gaseous mixture [19]. Normally, the substrate temperature to achieve the nitride layer is in a wide range from 673 K- 873 K [6]. However, working at lower treatment temperatures in plasma nitriding is the most important because of the obvious benefits of lower costs, low distortion of the workpieces [20], and maintenance of the nano and microstructure on the surface [21].

1.2 Purpose of This work

The main objective of this research is to explore the nitride layer on extrusion (Al2011) aluminium alloy, casting aluminium alloy (Al-6%wt), and H13 steel samples using the rf plasma nitriding process. In particular, surface hardness and nitride precipitation on the surface layer for varied treatment times in N_2-H_2 gas mixtures at low temperatures (below $400^\circ C$) are investigated. A significant problem of treated aluminium alloy is aluminium oxide (Al_2O_3) which prevents nitrogen atoms from diffusing into the sample. Therefore, plasma nitriding using the source at low pressure, it is expected that the oxidation on the aluminum surface is decreased.

To avoid low corrosion resistance [22] and the cracking tendency problem of the treated sample, temperatures below $450^\circ C$ are required. Hence, the possibility of employing lower substrate heating temperatures (below $400^\circ C$) was found in this work.

1.3 Scope and Thesis Organization

In this work, Al2011 aluminium (aluminium-copper alloy), aluminium copper 6%, and AISI H13 are chosen as substrate of nitride layer. The scope of study is forming of AlN layer on the aluminium alloy (Al2011, and Al-6wt %), and iron nitride on H13 by using rf-ICP nitriding. The analysis of this nitriding is evaluated by using Electron probe microscopy (EPMA), optical

microscopy, and x-ray diffraction. The scope of the dissertation also covers the testing of mechanical properties such as hardness. However, the type of testing focuses on EPMA which can confirm the diffusion nitrogen on sample.

This dissertation is divided into six chapters. The first chapter explains about the thesis motivation and objective of the work.

Chapter 2 provides the background information required for the work in this thesis. This chapter presents a brief introduction to the metallurgy of nitriding (including phase diagram, crystal structure, and etc), rf-ICP, and nitride layer, techniques for surface hardening, plasma nitriding mechanism, and previous studies.

Chapter 3 details the experiment methods employed throughout this study, including the investigated material, substrate preparation, and plasma nitriding procedure. In addition, reviews of the techniques used to characterize the nitride sample are included.

Chapter 4 examines the characterization results of the nitride layer on aluminum 2011 extrusion sample and the casting Al-6wt% sample.

Chapter 5 reports the parameter that can achieve the nitride layer of AISI H13. In addition, the effect of treatment time will also be examined with lower treatment temperature. At the end of chapter, the hardness of nitride sample will discuss.

Finally, chapter 6 is the discussion and conclusion of the work. The suggestion for future work is given.

CHAPTER II

REVIEW OF LITERATURE AND THEORETICAL BACKGROUND

2.1 Chapter review

This chapter reviews the theoretical background which is necessary for understanding and discussing of the results. Material including aluminium, aluminium alloy and H13 which used in experiment were begun to discuss in this chapter. The plasma nitriding knowledge including process, stages, important parameters, limitation, plasma source are briefly discussed.

2.2 Aluminium and aluminium alloys

Pure aluminium is a silvery white metal which is a light metal (2698 kg.m^{-3}) with a low melting point ($660.32 \text{ }^\circ\text{C}$) [22]. Aluminium was interested from industrial application because mechanical properties include ductile, malleable, and high good formability. Moreover, they exhibit good corrosion resistance because aluminium easily reacts with oxygen to form aluminium oxide (Al_2O_3) by the oxidation reaction. The typical thickness of aluminium oxide layer is 2.50 to 3.00 nm (25 to 30 \AA) at room temperature [23]. However, they still have mechanical strength problem. To solve the problem, adding alloying element such as manganese, silicon and copper can be used. Aluminium alloy contains different elements can be created a different mechanical properties for applications i.e. work hardening and annealing. They can be divided into two groups: wrought alloys (worked to shape) and cast alloys (poured in a

molten). For wrought alloys, the aluminium association's designation system used a four-digit number to represent for each element in alloy. The first number of alloy is shown the primary alloying element [24]. For some example in application, the 2xxx and 7xxx are suited for aircraft parts [25-26]. The aluminium and aluminium alloys are often call in term light metals because they are frequency used to decreased the weight of component. Nevertheless, the limitations of aluminium alloys are clearly presented in moving part of automotive application [27] because of their low surface hardness, lack good wear resistance. Therefore, surface hardening processes by aluminium nitrides coating are necessary for improving their properties.

2.3 Hot Work Tool Steels

Hot work steels are the metal that used in high temperature. The name of hot work is determined to include all applications excepting cutting tools that operating temperature rise above 200⁰ C [28]. Normally, hot work steels are mainly used for diecasting, extruding, hot pressing and hot-forging [28]. Because of their properties including hot yield strength, high temperature resistance, and toughness [28] which prospered for severe thermal and mechanical stresses. The above features are accomplished by adding alloying elements such as tungsten, molybdenum, chromium, cobalt, vanadium, etc [28]. H13 is also hot work steel which mainly contain chromium alloying [29]. However, this steel presents a relatively low wear resistance, but it can be improved through surface hardening treatment [3].

2.4 The nitride of metals

Nitrides of various elements play an important role in industry [30]. The addition of nitride in metals including boron, titanium, iron, molybdenum and aluminium (most metal in groups III, IV, V and VI) has aroused commercial interest because of their properties including the good corrosion resistance and electrical properties, high hardness, and wear resistance [13,31]. The comparison of physical properties between aluminium and aluminium nitride were listed in Table 2.1. The hardness of AlN is greater than Al. AlN ceramics are materials with high bending strength (300-400MPa) and Vickers hardness (12 GPa) [32].

Table 2.1: Physical Properties of Al and AlN [33]

| | Al | AlN |
|---|-----------|-------------------|
| Melting point [K] | 933 | 3273 |
| Density, ρ [g/cm ³] | 2.7 | 3.24 |
| Young 's modulus, E [GPa] | 72 | 320 |
| Hardness HV at load [N] | 20-30/100 | 1530/1 |
| Thermal expansion coefficient, α [10 ⁻⁶ K ⁻¹] | 23 | 4.7 |
| Thermal conductivity, η (max)[Wm ⁻¹ K ⁻¹] | 226 | 320 |
| Electrical resistivity, ρ [10 ⁻⁸ Ωm] | 2.5 | ~10 ¹⁹ |

AlN exist only one crystal structure (wurtzite, hexagonal) which is a stable compound in the binary system Al-N. The formation of aluminium nitride, nitrogen ion inserted into the aluminium matrix created widening of the Al Face-Centered Cubic (FCC) lattice, and then the hexagonal is gained [34]. The lattice constant of a and c are in the range from 3.11-3.11 Å⁰, and 4.98 - 4.98 Å⁰, respectively. Normally, colorless and transparent was found in pure AlN. On the other hand, AlN is easily colored by dopants and impurities, for example, light gray AlN was shown with

carbon participate [35]. Although, the hexagonal AlN phase is generally found but Moradshahi reported that Meletis and Yan have presented an fcc AlN structure [6].

The polycrystalline of metals and ceramic consist of many randomly oriented crystalline regions or grains [36]. An ultrafine grain size in the range of 3 to 100nm refers the nanostructure material, nanocrystals, or nanophase material [37]. The nanocrystal gain interest in researchers because they present an improved the mechanical and physical properties, e.g. increased mechanical strength, enhanced diffusivity, and electrical resistivity [38] in compare with the same polycrystals with conventional coarse-grain sizes. Tong et al. [39] used the gaseous nitriding to perform the nanostructured surface layer on iron matrix. The grain size of nanocrystallined with 20 μm thick was calculated an average grain size of 8 nm. The experiment result also reported a high hardness and excellent wear resistance. In addition, Quast et al. [11] have shown the nanocrystalline with hexagonal aluminium nitride AlN by using plasma nitriding on pure aluminium at treatment temperature between 460 $^{\circ}\text{C}$ and 535 $^{\circ}\text{C}$.

In plasma nitriding of steel, iron crystal structures present three form including BCC ($\alpha\text{-Fe}$), FCC ($\gamma\text{-Fe}$), and BCC ($\delta\text{-Fe}$) and relate with different temperature. After introducing nitrogen (N) into iron structure ($\alpha\text{-Fe}$), the new phases are formed including γ' -nitride (Fe_4N), and ε -nitride (Fe_{2-3}N). Moreover, when the nitrogen content exceeded 0.1%, the γ' -nitride was formed.

2.5 Techniques for the formation of nitride layer

Nitrides layer including AlN, CrN, TiN, and FeN can be achieved by several techniques such as plasma nitriding, plasma immersion ion implantation (PIII or PI^3), PVD, CVD, and etc, as shown in Fig.2.1. For improve the mechanical properties for automotive parts, the substrate treatment techniques are suitable more than layer additions techniques because of no cracking between modified layer and matrix of specimen. For substrate treatment techniques, the most of researcher not only interested to increase the hardness and thick layer of nitrided but also

investigated the improving wear resistance of nitrided steel. However, some literature review not directly measured the wear resistance because increasing hardness and nitrided layer thickness are implied to reduce of wear loss [40].

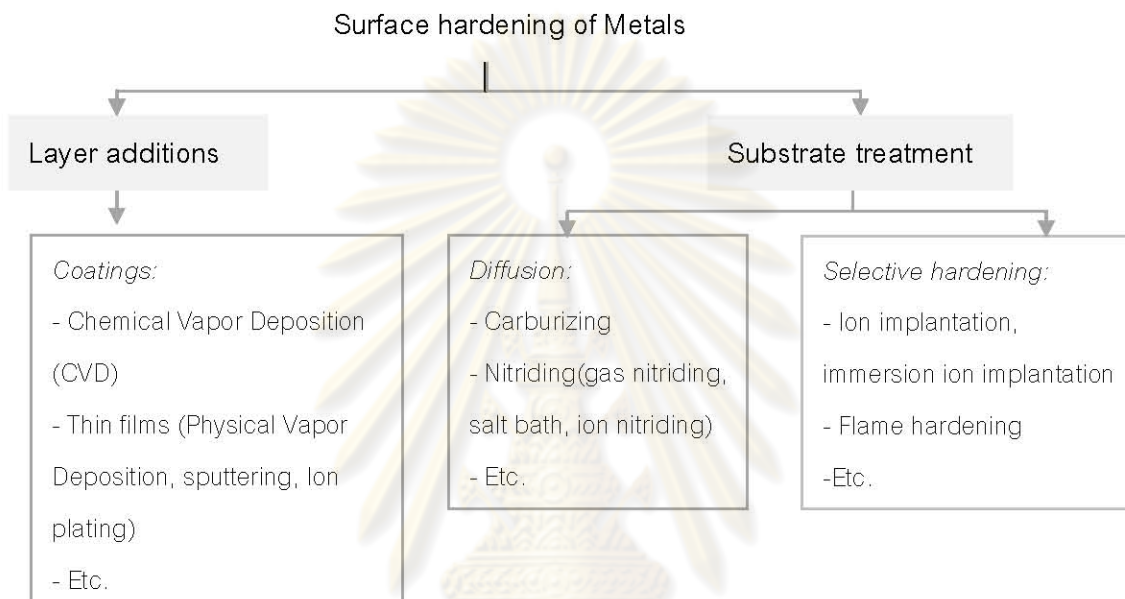


Figure 2.1: Diagram of engineering methods for surface hardening of steels [41]

2.5.1 Physical vapor deposition (PVD)

This method involves the sputter aluminium target in a reactive gas atmosphere. Nitrogen and argon are used as the discharge gas. After aluminium atoms were kick out from the metal (Al) target, and then combine to form a compound aluminium nitride (AlN) which deposit on the substrate including Si wafer, glass, and aluminium. The formation of AlN by PVD is also reported the hexagonal crystalline as same as a plasma nitriding technique. Additionally, the advantage of this technique is not required high temperature and heating substrate. Figueroa et al. [42] compared the AlN formation between plasma nitriding and PVD technique.

They found that the morphology of the treated sample PVD shows a smooth surface than plasma nitriding process, and the thick of nitride layer can produce in shorter processing time. However, the disadvantage of PVD, it was found that it cracks between modified surface and matrix as working on high load.

2.5.2 Chemical vapour deposition (CVD)

In this process, the activation energy is used to form a nitride layer. The activation energy for CVD mainly divides into two parts: thermal activation and plasma activation. In thermal CVD, high temperature ($>900^{\circ}\text{C}$) is required to activate the reaction [43]. A typical thermal CVD system consists of gas system, reactor, and deposition chamber. For plasma CVD, the working temperature (300 to 700°C) is less than thermal CVD [43]. However, the disadvantage of this technique is the stress of nitride layer due to thermal expansion at high temperature.

2.5.3 Plasma immersion (ion) implantation (PII)

Surface modification by ion implantation process uses very high energy ions in the range between 10 and 500 keV [41], which can implant into the surface. In PII technique is required high specification equipments i.e. high voltage generator, and high vacuum to avoid the scattering of the ion beam [44]. Moreover, the Al_2O_3 is not a critical problem for the formation AlN because the high energetic ions can break the oxide film and then penetrate into the Al substrate. For example of this technique, Sonnleitner et al.[45] reported that AlN layer was performed using PI^3 treatment at accelerate voltage up to 20 kV at pressure 1.2×10^{-3} torr for 2 h. They reported that the layer thickness of AlN is approximately 30-60 nm at rf power in the range 300 to 1000 W, for treatment time 4 h, and the thick of nitride layer between 50 and 60 nm. Blawert et al. [46] investigated that PII technique cannot form nitrides on Al 99.5 at

temperature below 500°C. However, they found that nitrogen was found but layer cannot be formed. Therefore, the hardness and wear resistance cannot improve under their condition.

2.5.4 Traditional nitriding methods

Nitriding is a heat treatment technique which is involved diffusion of nitrogen to perform a nitride layer into aluminium or steel alloys. The process is carried out at a temperature between 500° C- 575 °C in different medias. High temperature is required because nitrogen easily diffuse by vibration amplitude. The mechanism of nitriding is well known. The specific reaction depended on several factors including the type of alloys and the nitriding media. The precipitation of nitrogen is referred to the hardening of the surface layers which is also related the case depth of nitride layer. A typical AlN layer is normally found in hardening of aluminium. For nitriding of steel, the typical nitrided component can be divided into two parts: compound layer or white layer; and diffusion layer. The nucleation growth areas will eventually become the “compound layer” or commonly call the white layer (refer to white color after polished etched surface) which can form up to a different structure, single-phased Fe_4N (γ -phase) or the single-phased $\text{Fe}_{2,3}$ (ϵ -phase), and mixture of the two structure [28]. The white layer has a good hardness but it is brittle. However, it's not good for long lifetime. To eliminate the white layer, it is used adding Ar during plasma nitriding [47] or adjusting the amount of nitrogen [48]. Moreover, Rolinski reported that the compound zone thickness can be decreased by increasing nitriding time. Due to the short nitriding time process, carbon atoms were diffused to the specimen surface by reacting with nitrogen and iron atoms, and helping the formation of ϵ -phase. Increasing nitriding time, the surface was decarburized while carbon was sputtered away and replaced by nitrogen [49]. Then, the nitride phases were shifted to gamma prime cause by a small amount of carbon atoms in specimen. In the diffusion zone, this layer is beneath the compound

zone containing precipitated alloy nitrides [50]. The depth of diffusion zone depends on the ion nitriding temperature [28] and also the chemical position of the steel.

The three main media of nitriding are based on gas, salt bath, and plasma. Gas and salt bath nitriding, are still used in commercial, but they are highly toxic and unfriendly environment. Gas nitriding is a process that used a source of nitrogen includes NH_3 , $\text{NH}_3\text{-H}_2$ mixtures, NH_3 mixed with an endothermic gas, and $\text{NH}_3\text{-N}_2\text{-CO}_2$ mixtures [51] for forming AlN precipitates. In this process, the forming nitride layer can be distinguished into two sections: diffusion of nitrogen carrier (ammonia) towards the iron surface, ammonia adsorption and dissociation on the surface, and; nitrogen absorption and dissociation into the surface [52]. The temperature above 500°C plays an important role in increasing the case depth of nitride [28]. However, the type of composition is also affected to the desired hardness and case depth. In this method, the disadvantage of gas nitriding are long period of time (typically 20 to 80 hours), fatigue strength, etc. Moreover, gas nitriding of aluminium is difficult to form AlN because nitrogen doesn't have enough energy to break the aluminium oxide bond and diffuse into aluminium matrix.

Salt bath nitriding is nitriding techniques which use the treatment temperature in the range $560\text{-}580^\circ\text{C}$. And, the case depth is typically of the order of 0.05 mm or less [53]. In this process, the reaction relate with the oxidation of the cyanide to cyanate which can dissociate to release nitrogen for diffusion to the surface [53]. A typical salt bath in nitriding is composed of sodium cyanide, sodium cyanate, sodium carbodate and alkaline chlorides which are very toxic material [53-54]. Therefore, plasma nitriding is preferred to surface modification because no toxicity.

2.5.5 Plasma nitriding process

Plasma is a fourth state of the matter which is a collection of neutral gas atoms and molecules, charge particles in the form of positive ions, negative ions and electron, and photon [55]. The most common known to people in examples of plasma are interstellar gas, star, stellar atmospheres and lighting which is occurred in neural. Moreover, plasma can generate in laboratory by electrical discharge. An example of electrical discharge is occurred in the vacuum tube with consist of parallel two electrode and small amount of gas. Voltage is applied by driving an electric current through it, which make the ionization gas, and emit light in the red and blue color range which depend on the type of gas discharge. However, the classifications of plasma are distinguished by electron energy kT_e and electron density with several types of plasma in nature and laboratories. Plasma is sometimes referred to as ionized gases which have a many different methods of creating plasma in laboratory, and plasma may have high or low density depending on plasma source.

An ionization process is required the energy source to convert the atom or molecule into a positive ion and also electron. The main two participants of the ionization process, electrons and positive ions, are the most important charge particle in plasma. Electrons are the first particles in receiving energy from electric field and then transmit the energy to all other plasma components, providing ionization, excitation, relaxation and recombination [56]. Consider the positive ions, they are occurred after the atoms or molecules lose their electron in ionization processes. The positive ions are a heavy particle and can't directly relieve energy from electric field because of collisional energy exchange with other plasma components. However, in low pressure discharge, the ion energy can be quite high cause by electron impact the heavy particle with inelastic collisions. The result after collision is that the energy was transfer from kinetic energy of collision partner into internal energy. Moreover, the important parameters using to characterize plasma are plasma density (n) and the temperature T of each species

i.e. ions, electrons and neutrals have a different temperature: T_i , T_e , T_n . Moreover, a host of subsidiary parameter (e.g., Debye length, plasma frequency) can be derived from n and T parameters [54]. Normally, Langmuir probe was used for the characterization of basic plasma parameters such as plasma density and electron temperature.

Plasma nitriding (PN) also known as ion nitriding or glow discharge PN [57] is a thermo-chemical technique that can use for improving surface hardening, corrosion, and wear resistance of non-ferrous (including aluminium alloy, titanium, etc.) and ferrous material (including hot working tool steel, stainless steel, etc.) which in general enhance the fatigue life of components. This technique was developed in the early 1930s by Egan and Berghaus [58] as an alternative to the gas nitriding process. Plasma state that use in plasma nitriding can be generated by electric discharge or rf discharge. This process requires the vacuum system include vacuum pump, mass flow controller, chamber and so on, to ignite the plasma. The pressures that use in DC and rf plasma nitriding are in the range 1- 8 torr and lower 1 torr. Fundamentally, ion nitriding is done in the low pressure chamber in which mixtures of hydrogen and nitrogen gases discharge [28]. The process requires vacuum system for removing the contaminating gases. Moreover, plasma nitriding is operated at low pressure and high voltage because affect the ionization efficiency and flux energies, which is much higher than conventional plasma. The plasma source including DC and rf are usually used to nitrogen and hydrogen glow discharge, which is represented a blue-violet glow around the samples being treated. The charged positive (nitrogen) ions are accelerated and impinged the workpiece. The ion bombardment leads to heat the workpiece, cleans the surface, and provides active nitrogen [48].

Normally, nitriding process of aluminium alloy consists of 2 step; pre-sputtering, nitriding. The pre-sputtering process is used for cleaning and eliminating the contaminated substrates before nitriding which sometime call pre-treatment process. This process is very important for

aluminium alloy which has a thin oxide layer cover on matrix. Because of aluminium oxide layer is prevented to form the nitride layer, therefore sputter before nitriding is necessary. The factor including ion energy, ion mass, substrate temperature, incidence angle, alloying elements are the effective parameter for sputtering yield or sputtering process [59]. Normally, the argon gas was used to sputter the oxide film. Because aluminium alloy consist of various elements such as Cu, and Mg. Moreover, the sputtering yield of Al_2O_3 is less than that yield of aluminium, it cause Al easily etch and make the surface roughness [60]. Therefore, the roughness of nitride surface was always observed. Moreover, after nitriding, the Al_2Cu is easily participated on the surface because high sputter yield compare with aluminium. However, Al_2Cu can reproduce for helping the AlN formation that follow solid state reaction by $\text{Al}_2\text{Cu} + 2\text{N} \rightarrow 2\text{AlN} + \text{Cu}$ and $2\text{Al (in matrix)} + \text{Cu} \rightarrow \text{Al}_2\text{Cu}$ [27].

However, plasma nitriding of steel is not required pre-treatment because sputtering process by ions sputter is enough to eliminate the contamination on specimen. Most of studied in plasma nitriding have reported the large of CrN participate at treatment temperature over 450°C , but Kim et al. [20] found that CrN formation can observe at 400°C . This is due to the reason that the different alloys show the transformation at different temperature. Michel et al. [61] also studied in plasma nitriding of aluminium alloy. They found that hydrogen admixture during sputtering process can reduce the surface roughness and effectively decreases the oxygen content of the surface. It can be explained that addition of hydrogen as pre-sputtering process not only decreased the energetic ions bombardment of argon but also the chemical etching is helped to eliminate the Al_2O_3 . For this reason, the gases include argon or mixers Ar- H_2 are normally used for pre-sputtering process. At the end of pre-sputtering process, the specimen was heated by heater; typically temperature is 520°C . Nitrogen or nitrogen-hydrogen mixers were used in this process. Then, the interaction between the plasma and substrate result in the formation of nitride layer on the substrate.

The principle mechanisms include sputtering and re-deposition for plasma nitriding of steel is showed in Figure 2.2. The N ions sputter the specimen surface, and then the atoms of elements within specimen (including Fe, Cr, Mo, and other non-metallic elements such as O and C) are removed from the surface. Thereafter, the removed atoms (mostly Fe atom) are combined with the reactive N in the plasma to form iron nitride and then recondensed onto the surface (FeN_x). The iron nitride was dissociate and allows the diffusing nitrogen into the surface at nitriding temperature [62].

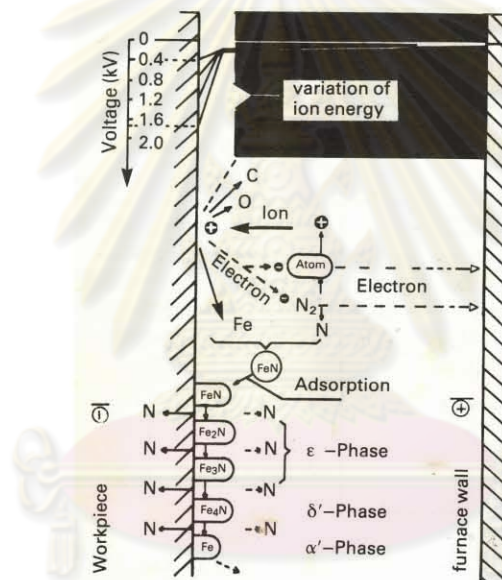


Figure 2.2: Model of iron nitriding in DC plasma nitriding

ศูนย์วิจัยทรัพยากร
จุฬาลงกรณ์มหาวิทยาลัย

2.6 Emission spectroscopy of gas discharge in plasma nitriding process

Novi Granito [40] concluded that the nitride layer using plasma nitriding can form on sample by two reactions, including the absorption of reactive species, and the diffusion of nitrogen. Therefore, plasma diagnostic is important obtained. The optical spectroscopy is best equipment to obtain the reactive species responsible for nitriding. In N_2 - H_2 plasma, it was found that many excited species such as N , N^+ , N_2 , N_2^+ , H and N_iH_j ($i=1, j=1\sim 5; i=2, j=2$) [40] in the mixed H_2 and N_2 plasma. In DC plasma nitriding, N_2^+ emission was detected to be the most intense in the negative glow of N_2 and N_2 - H_2 at pressure plasma at 1.5-2.2 torr using emission spectroscopy [61]. The excited species including N^+ and N_2^+ are a sputter ion, which can produce nitrogen and iron atom as show in Fig.2.3. The presence of those sputter ion can increase a surface roughness for long treatment time. However, N^+ and N_2^+ species can react with the specimen surface to proceed the nitriding reaction [40]. In addition, NH and H radicals that produce in N_2 - H_2 plasma nitriding, play important role in nitriding. Because of H radicals may convert the NH radical to an active nitrogen atom [62] and diffuse into the specimen.

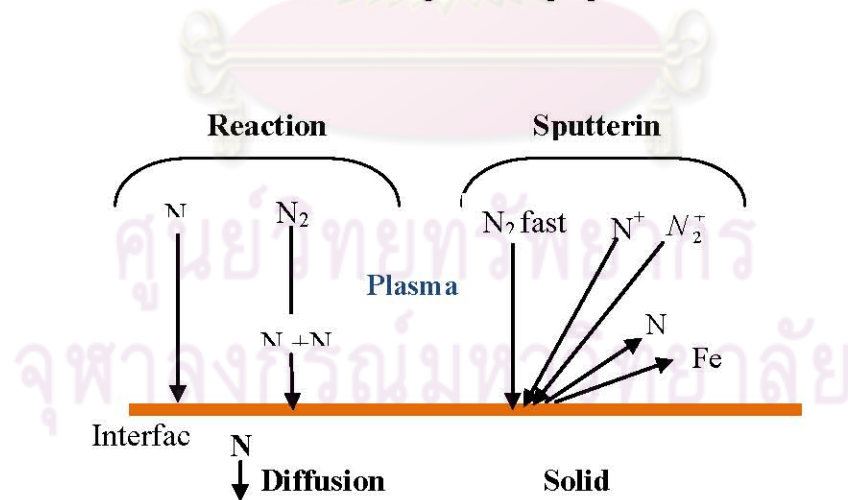


Figure 2.3: Phenomena influencing the atomic nitrogen concentration at the surface of an iron or steel sample during plasma nitriding [52].

2.7 Power source to plasma nitriding techniques

The power source DC and rf are normally used to generate plasma. At the beginning in plasma nitriding, DC source is mostly used for plasma glow discharge because of simple and inexpensive [63]. However, this source has a problem about contamination from electrode inside the chamber. For avoid that problem, some researchers are changed the power source to radio frequency (RF) plasma generation which is the environment friendly and high plasma densities with relatively leading to faster processing. The wide applications of rf-ICP are due to following: contamination free, flexible choosing plasma gases [64], and less gas consumption [65].

2.7.1 DC plasma nitriding

For many years, plasma nitriding has been carried out by DC power supply to generate a plasma glow discharge caused by the ionization of gases. This method mainly consists of two electrodes inside the chamber. The typical apparatus shows in Figure 2.5. Heater is used a resistive heater place under the sample holder. Typically substrate temperature ranging from 350- 580°C [4, 65] is commonly in DC plasma nitriding. The usually working pressure is carried out at between 0.75-7.5 torr with a 0.3-1 kV substrate voltage [61]. The sufficiently high DC voltage is applied between the two electrodes then the current is flow between them. The charge particle including negatively electron and positively ion are moving toward to positive electrode (anode) and negative electrode (cathode), respectively. Then, the nitrogen ions react with the specimen present forming nitride layer on matrix. As it is well known, the thickness of nitride layer depended on various variables such as type of material, heat treatment temperature, and treatment time. Table 2.2 shows some examples of the processing parameters in difference materials include aluminium and AISI H13. From this Table, it can be

seen that the thickness of aluminium nitrides are much less than those of iron nitride. To explain this, because of the incompletely removing aluminium oxide (Al_2O_3) on aluminium alloy after pre-sputtering process and residual chamber oxygen in chamber cause to reform oxide on surface with inhibit to perform a nitride layer.

Table 2.2: Summary of experimental conditions for DC plasma nitriding from published literature

| Material | Voltage(V) | Working P (torr) | Time (h) | Temp. (°C) | Substrate Bias(V) | Thickness (μm) | Ref. |
|--------------------|------------|---------------------|----------|---------------|----------------------|--------------------------------|------|
| Pure aluminium | NR | 4 | 20,40,70 | 550 | -200 | 2-3 | [12] |
| Al1100, Al 2025 | 700 | 0.6 | 20 | 400 | NR | 2.2 | [66] |
| H13 | NR | 3 | 10 | 380 | NR | 65 | [67] |
| H13 | 380 | 3 | 36 | 400 | NR | 66.8 | [68] |
| H13 | NR | NR | 20 | 500 | -200 | 113.6 | [69] |

*NR=Not Reported

2.7.2 rf plasma nitriding

The rf-ICP discharge is more efficient over DC discharge which is represented in parameters as shown in Table 2.5. In addition, DC glow discharge is lower ionization than rf discharge, because of the mechanism about electrical break down in DC. Initiating electron cause to either electrons by collisional ionization or secondary process, or the second electron was produced from electrode which is different in rf discharge. From rf discharge, electrons will not losses for drifting to electrode, and not require the secondary emission process at the electrode for maintain of the discharge. Basically of rf-ICP discharge, high frequency electric

current passed through a solenoid coil providing an axial magnetic field, which induces the vertical electric field sustaining the rf-ICP discharge [56]. Then, the field will couple to electrons; produce ionization by electron collision, and keep to sustain the discharge. Moreover, the common accessory in rf-ICP is a matching network that use to increase the power dissipation in the discharge, and to protect the generator. In figure 2.6b is shown the schematic circuit of rf-ICP discharge. A long solenoid coil wind over the glass tube of radius R. The oscillating magnetic field of the rf current in the coil is sustain the discharge which can explain by Maxwell equation. The proportional electric field which is accorded with Maxwell equation requires the frequency between 0.1 MHz and 100 MHz. Typically rf plasmas are operated at 13.56 MHz because of the interference avoidance with radio communication system, which is international frequency using industries and laboratory.

The pressure of chamber affect the to ion energy in rf discharge with relatively in plasma nitriding process. Fig.2.4 show the relation between pressure and ion energy. It can be seen in figure that, the decreasing pressure produces a increasing of ion energy. Because of the mean free path are inversely proportional to pressure (equation 2.1), low pressure can rise the higher energy ion flux to substrate surface. The equation of mean free path (MFP) is calculated from:

$$\lambda = \frac{1}{n\sigma} \quad (2.1)$$

Where n is the density of the particle and σ is the collision cross-section of the particle. From this equation, the effect of pressure is following:

$$\lambda \propto \frac{1}{p} \quad (2.2)$$

Therefore, high pressure (short MFP), ions have more collision which decrease energy of ions to diffuse on specimen.

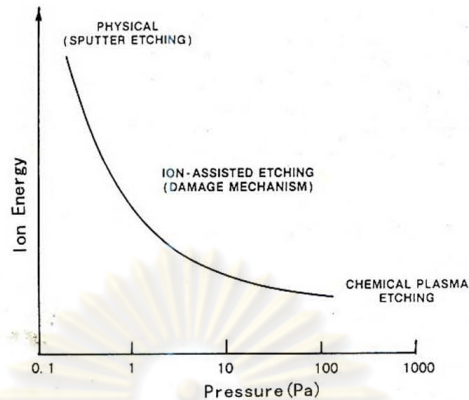


Fig.2.4: Graph of ion striking decrease and the flux of neutral radicals increase with pressure [70]

The radiofrequency (rf) is widely used in fabrication of micro-electric device, and in modification of surface materials. The glow discharge of rf plasma with produce with high frequency is divided into two parts: Capacitively couple plasma source (CCP) and inductively couple plasma source (ICP). In CCP source is consisted of two metal electrodes separated by a small distance, the discharge is ignited between electrodes by radio frequency (rf) power supply, which the upper electrode is connected to the power supply and another one is grounded, represented in figure 2.5a. In this work, rf-ICP was used to ignite the plasma using electromagnetic induction, as shown in Fig. 2.5b.

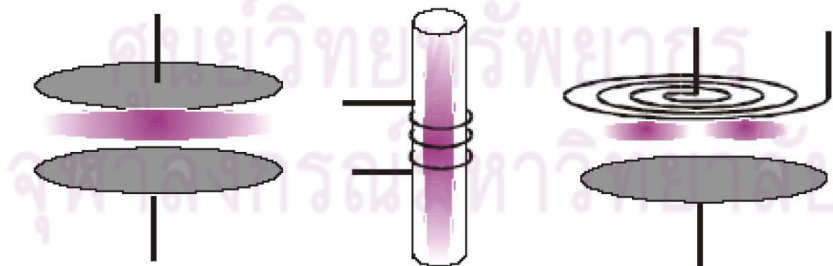


Figure 2.5: (a) Typically CCP discharge, (b) ICP discharge with helix, and (c) ICP discharge with planar antenna [71].

Basically, rf- ICP exists two mode transitions: E-mode (electrostatic mode) and H-mode (electromagnetic mode). In the E-mode or bright mode is referred to low electron number density. By increasing the RF power (increasing the induction coil's current), the mode can change from E-mode to H-mode with relatively increased electron number density. The rf-ICP discharge is mostly depended on rf power, gas mixture, and gas pressure. Therefore, H-mode is benefit for plasma nitriding. Because of the higher electron density is related to the higher ionization efficiencies with significant in reducing nitriding time. However, nitrogen discharge in rf plasma, Czerwiec et al. [72] reported in their work on nitrogen dissociation in a low pressure cylindrical ICP discharge that at relatively higher pressure, the discharge is stable but does not produce intense nitrogen atom emission. They also reported that the brighter mode (H-mode) is localized at the center coil position and only E-mode discharge can be observed at relatively lower power. Moreover, the comparison with dc discharge is presented in table 2.3. Form this table, it can be seen that rf glow discharge is good characteristics about electron energy, electron temperature, and higher plasma potential. Moreover, the high electron temperature in rf source is related to kinetic energy of the electron which is significant to rise the ionization and excitation of neutral N_2 molecules, and enhances the nitride layer on aluminium substrate.

ศูนย์วิจัยทรัพยากร
จุฬาลงกรณ์มหาวิทยาลัย

Table 2.3: Comparison of plasma parameters in different power source using Langmuir probe [73]

| Parameter | rf | dc |
|--|---|---|
| Electron density(cm^{-3}) | 2×10^{10} to 6×10^{10} | 2×10^{10} to 18×10^{10} |
| Average electron energy(eV) | 4 to 7 | 0.7 to 1.0 |
| Electron temperature(eV) | 1.5 to 2.5 | 0.2 to 0.6 |
| Ion number density(cm^{-3}) | 3×10^{10} to 12×10^{10} | 4×10^{10} to 20×10^{10} |
| Plasma potential (eV) | 9 to 16 | 2 to 4 |

In order to obtain the rf-ICP plasma nitriding process, the procedure is similar to dc plasma nitriding. But the experiment condition is different depend on the characterization of rf source. Table 2.4 shows the example of plasma nitriding condition in published literature. By doing this process, the nitride layer can achieve at shorter treatment time and low working gas pressure. However, it has been clearly seen that aluminium alloy is still hard to perform aluminium nitride layer, even though the plasma source is different.

Table 2.4: Summary of experimental conditions for RF plasma nitriding from published literature

| Material | rf (W) | Power | Working Pressure (torr) | Time (h) | Temp. ($^{\circ}\text{C}$) | Substrate Bias(V) | Thickness | Ref. |
|-------------------------------|-----------|-------|----------------------------|----------|---------------------------------|----------------------|---------------------|------|
| Al2011 | 100 | | 0.05 | 3 | 400 | - | 15 nm | [9] |
| Al2011 | 100 | | 0.0025 | 3 | 575 | -400 | 2-3 μm | [74] |
| AISI304 stainless steel | 300 | | 0.037 | 5 | 470 | -300 | 10-11 μm | [75] |

2.8 Influence of processing parameters on plasma nitriding

2.8.1 Addition hydrogen in plasma nitriding

A major problem in plasma nitriding of aluminium alloy is the oxide layer of Al_2O_3 which prevents the nitrogen atom from diffusing into the aluminium substrate. In order to eliminate aluminium oxide on surface, argon plasma etching can be successfully performed [15]. Moreover, additive of H_2 in pre-sputtering and nitriding had effect to temperature of substrate, because hydrogen molecule have a high energy ionization potential of 15.43 eV which can change the electron temperature that effect to substrate temperature [76].

As claimed by other researchers, adding hydrogen during the sputtering can significantly improve the formation of nitrided layer by eliminating of oxygen from the surface [77]. However, the role of adding nitrogen in nitriding process has a different opinion. Renevier et al. [78] reported that addition of hydrogen gas to nitrogen has no effect in dc plasma nitriding at gas pressure in range 3×10^{-3} torr to 7×10^{-3} torr. On the other side, Negm concluded [79] that the addition of hydrogen up to 50 % might improve plasma nitriding efficiency and properties of the treated sample; in the other hand, adding hydrogen exceed 70% of total gas, it can retard the nitriding process. The other report is explained by Marchand et al. [80]. They found that addition 5-10% of H_2 lead to increase the discharge current in dc plasma nitriding which is due to the increasing of the secondary electron emission coefficient. Moreover, the addition of small quantities of H_2 is significant to increase the surface temperature which effect to form nitride layer with discussion in 2.6.2. The surface temperature can calculate by using the Boltzman law (eq.2.5) with the OES results. The surface temperature with corresponded to discharge current for several N_2 - H_2 mixtures at 2.6 torr in DC plasma is shown in table 2.5 [81]. From this table, addition hydrogen between 10 and 20 % in the total gas is clearly seen the increasing the current discharge which is correlated with the surface temperature.

Table 2.5: Surface temperature (T_k) for different quantitative of H_2

| H_2 | $T_k(K)$ | I (mA) |
|-------|----------|--------|
| 0 | 720 | 62 |
| 10 | 830 | 90 |
| 20 | 810 | 90 |
| 30 | 790 | 85 |
| 50 | 740 | 75 |
| 60 | 720 | 70 |
| 70 | 680 | 60 |
| 90 | 550 | 38 |

2.8.2 Effect of plasma treatment time

After plasma nitriding of aluminium alloys, two phases can be occurred including AlN and Al_2Cu . The interfacial boundaries of their phase are the part of nitrogen to diffuse into the matrix. At short treatment time, the large grain is show which is limited the diffusion of nitrogen. Therefore, in order to increase the nitride layer, long treatment time are require because it can increase the small grain size [6] and the interfacial boundaries which is increased the area for nitrogen diffusion.

2.8.3 Effect of heat temperature

As it well known, the case dept of nitride layer is mainly depended on the treatment temperature and treatment time. The heat system for substrate temperature is mostly used in electric heater which located under the specimen. By doing this heater in rf plasma nitriding, it is not suited because can cause significant perturbation as ion bombardment. Moreover, the electric or resistive heater is the short lifetime of the heating element and unsuitability for high

pressure sputtering and necessity of high pressure [82]. Ceyan et al. designed the radiative substrate heater using a 250 W halogen bulb which was installed into paraboloid-shaped cavity inside a brass block. This heater can reach to 800°C substrate temperature. For avoid the perturbation on rf discharge, we also used radiative substrate heater in this work. In relation between nitride thickness and nitriding temperature, Czerwiec et al. [83] obtained the diffusion layer thickness as the following equation:

$$\langle x \rangle \approx \sqrt{2Dt} \quad (2.3)$$

$$D = D_0 \exp\left(-\frac{E}{kT}\right) \quad (2.4)$$

Where $\langle x \rangle$ is the diffusion layer thickness, t is the process time at temperature T , D is the diffusion coefficient for N atom into the material and E (eV) is the activation energy for the diffusion process. In the above equations, the thick of diffusion layer is directly depended on increasing the treatment time and temperature. In addition, at high temperature of nitriding process, the diffusion coefficient of N atom is increased which made the nitrogen diffusion rate into the matrix [12]. In addition, for plasma nitriding of steel, FeN and CrN are usually found in the diffusion zone. As deeper form the surface, the Cr concentration is must larger than N concentration because of high diffusion coefficient, as compared in Table 2.6.

Table 2.6: Diffusion coefficient of nitrogen and chromium at several temperatures [84]

| Diffusion Coefficient | Temperature | | |
|--------------------------------|-------------------------|-------------------------|------------------------|
| | 773 K | 823 K | 873 K |
| $D_{N}, \text{cm}^2/\text{s}$ | 0.33×10^{-7} | 0.687×10^{-7} | 1.305×10^{-7} |
| $D_{Cr}, \text{cm}^2/\text{s}$ | 0.136×10^{-13} | 1.323×10^{-13} | 9.92×10^{-13} |

CHAPTER III

EXPERIMENTAL TECHNIQUES

3.1 The materials investigated

In this work Pure Al, 2011 aluminum alloy, Al- 6wt%cu, and AISI H13 were used the substrate material for plasma nitriding. Al 2011 was used in this experiment which is available in Thailand. The Al-6wt%cu is a die casting alloy from metallurgical engineering department from Chulalongkorn University. The chemical composition of the hot working tool steel H13 and the commercial grade of 2011 aluminum alloy are given in Table 3.1.

Table 3.1: The chemical composition of Al2011 and AISI H13 (wt %)

| Al2011 | | | | | | | | |
|----------|------|------|------|------|------|------|------|------|
| Al | Cu | Pb | Bi | Fe | Si | | | |
| Balance | 5.70 | 0.39 | 0.41 | 0.16 | 0.12 | | | |
| AISI H13 | | | | | | | | |
| Fe | C | Cr | Mo | Mn | Si | P | S | V |
| Balance | 0.35 | 5.10 | 1.14 | 0.40 | 1.10 | 0.02 | 0.02 | 0.96 |

3.2 Substrate Preparation

The 12 mm diameter cylindrical rod of AISI H13 was heat treated at 1000 °C and quench in air. After that, it was cut into a disk shape of 2 mm thick. Pure Al, 2011 aluminum alloy and Al-cu 6% plates with the size of 2 mm thick and 12 mm in diameter were also used as a sample.

All samples were ground using the silicon carbide grit number 400, 600, 800, 1200, and 2000 respectively then polished using 1 μ m diamond pastes. Finally, the samples were cleaned in acetone and then dried with hot air.

3.3 Nitriding Equipment

In this thesis, plasma nitriding is carried out by rf-ICP. The photograph and schematic diagram of the plasma nitriding is shown in Fig. 3.1. The plasma nitriding apparatus consist of (1) vacuum system, (2) gas supply, (3) matching network, (4) rf source, (5) gauges pressure, (6) temperature controller, (7) gas controller, (8) DC power supply, (9) electrically connecting, (10) cooling system. The system is based on the configuration of inductively coupled plasma (ICP) reactor. The 13.56 MHz 1,000 W rf generator (Dressler Cesar 1310), impedance matching network and planar coil antenna were used to couple rf plasma to plasma gases through the quartz plate. Ar, N₂, and H₂ of high purity grade (99.999%) were used as plasma gases. The amounts of gases fed into nitriding chamber were controlled by mass flow controllers. Part of heater, this work used a radiation heater from a 250 w halogen bulb which is placed directly underneath the substrate holder. The heating source connects with micro temperature controller unit (JCS-33A) which used to control the substrate temperature from 200 - 500°C. This controller measures the temperature by using a K-type thermocouple. To maintain the substrate temperature at a desired level, water could also be pumped into the cooling line circulated around the substrate holder. The power supply of the GW Instek GPR-30H10D (GPR-H Series) and GPR-60H15D which had a maximum output 300 volts and 700 volts respectively was used to bias the substrate to attract the ions.

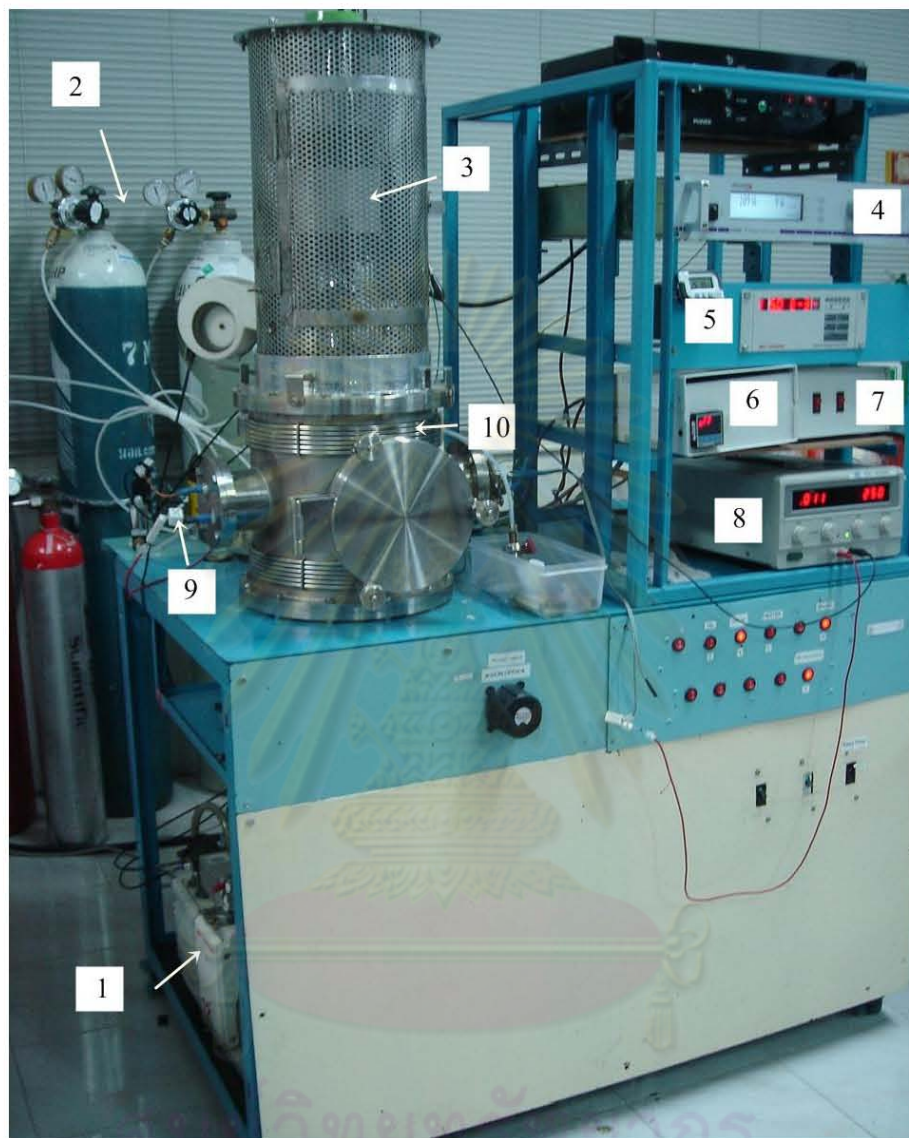


Figure 3.1: The plasma nitriding system as installed at plasma laboratory

3.4 Nitriding procedure

Plasma nitriding experiment was mainly carried out in the 3 step; preparation (polishing and cleaning), plasma nitriding (pre-sputtering, and nitriding), and cooling. For plasma nitriding step, the chamber was evacuated to base pressure at 5.5×10^{-5} torr using rotary and turbo molecular pump, respectively. Then, the substrate was heated by radiative heating source to the desired temperature. The pre-sputter started after introducing argon and hydrogen in to the chamber and ignition plasma. The holding time of 0.5 – 1 h in pre-sputtering process was used in experiment for removing the aluminium oxide. After finishing pre-sputter process, the chamber was evacuated to base pressure again. The plasma including nitrogen and hydrogen was introduced in the chamber. Then, heating of the substrate to the desired temperature, ignition plasma, and biasing the substrate were used in plasma nitriding steps. For each samples, the detailed of the plasma nitriding parameters are provided within the chapter 4, 5.

3.5 Nitriding conditions

For rf plasma nitriding of Al 2011, the process can be performed in two sub processes which are pre-sputtering and nitriding. In pre-sputtering process, the rotary pump was used to evacuate the system to the pressure of 2×10^{-2} torr, and then further by diffusion pump to 5.5×10^{-5} torr. The sputtering gas, Ar and, in some cases, Ar-H₂ admixture, was introduced to the chamber while the pressure was maintained at 1 torr. During the sputtering process, the rf power was fixed at 100 W while the substrate negative bias could be varied from -100 to -400 V. After sputtering process, the plasma nitriding took place by evacuating the chamber again until pressure in chamber reach base pressure at 5.5×10^{-5} torr. The aluminium substrate was heated by halogen bulb until its temperature reached the set values. Then N₂ and H₂ gases were introduced into the chamber at controlled partial pressure ratio of desired value. The total

pressure of the system is maintained at 1 torr. The rf power was set between 100 - 300 W while the different substrate bias voltage from -100 to -400 V were applied. The nitriding process would continue to the desired duration during which time the temperature was controlled to within 10 °C of set value. After nitriding process, samples were let to cool down in N₂ atmosphere for 1 hour. However, the conditions and experiment details will be explain in chapter 4, and 5, respectively.

3.6 Characterization Techniques

In this study, microstructures, compositions and hardness of the formation on the aluminium alloy and H13 substrates due to the rf plasma nitriding were analyzed by using various kinds of analytical techniques. The surface morphologies of the nitrated substrates were imaged using scanning electron microscopy (SEM) [JEOL JSM-6480LV]. An atomic force microscopy (AFM) [Veeco NanoScope IV] was used to investigate the angstrom-scale surface roughness of the samples. Nitrogen distribution after plasma nitriding was observed by electron probe microanalysis (EPMA) with wavelength dispersive x-ray analysis (WDX) method. In addition, the crystal structure of the AlN was investigated by grazing incidence x-ray diffraction (GIXD) [Rigaku TTRAX III] using Cu K α radiation. The surface hardness was determined by nano-indentator using a North Star indenter tip.

3.7 Morphology and Composition

3.7.1 X-Ray Diffraction analysis (XRD)

X-ray diffraction is a powerful, non-destructive technique that exposes the quantitative and qualitative analysis of the material including composition, lattice constant, crystal structure, crystallite size, and so on. Bragg's law in equation 3.1 can be used to explain the interference

pattern of x-ray scattered by crystal. Fig. 3.2 shows the incident angle and reflected (or diffracted) ray during the incident X-rays impinging the sample.

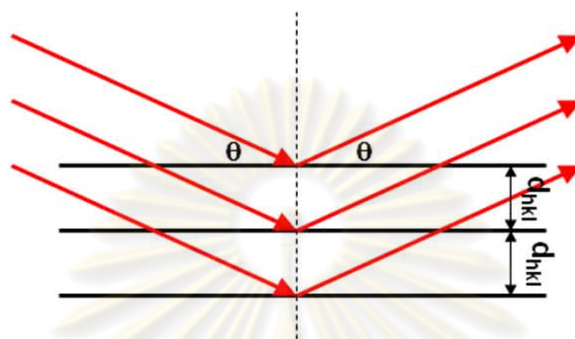


Figure 3.2: Diagram of x-ray diffraction

$$\lambda = 2d_{hkl} \sin \theta \quad (3.1)$$

Where λ is x-ray wave length, θ is x-ray incident angle and d is lattice spacing of atomic planes. In this study, XRD was carried out on JEOL (JDX-3530) and Rigaku TTRAX III diffractometer, using $K\alpha$ radiation ($\lambda = 1.5406 \text{ \AA}$). The JCPDS database was used to identify the x-ray peak. The XRD equipment consists of three main components: an x-ray tube, a sample holder, and x-ray detector. The electron from heating filament was accelerated to collide the copper anode by applies a voltage, and then the x-ray was emitted. These x-rays are collimated and directed on to the sample. During this process the sample was collided with a two different geometries: Bragg-Brentano (XRD) and Grazing incidence x-ray diffraction (GIXRD), as shown in Fig.3.3, and Fig.3.4, respectively. Bragg-Brentano geometry is shown the diffraction pattern for a movable sample holder and detector. In the contrary, GIXRD geometry is shown a bit moving of detector as x-ray incident (a few degrees) into the sample. For the report part, the diffractogram is in the form of the scattered of x-ray intensity (counts/s and log) versus 2θ (degree).

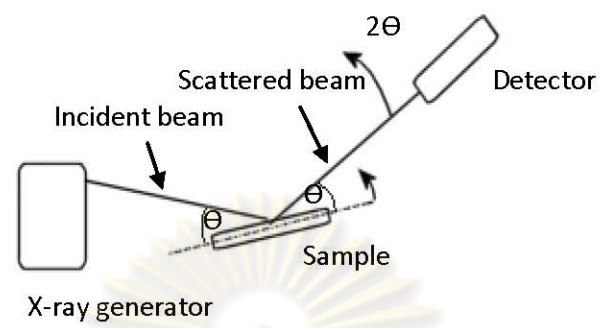


Figure 3.3: A Geometry of the Bragg-Brentano method.

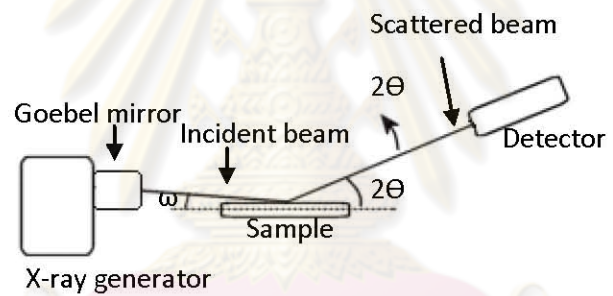


Figure 3.4: A Geometry of the GIXRD method.

Moreover, XRD result can be used to estimate the crystallites size of nanophase material by the observed line broadening. This knowledge was published in 1918 by P. Scherrer namely Scherrer's formula. The broadening peak is described by D, which is the full width at half maximum (FWHM) intensity of the peak.

$$D = \frac{0.94\lambda}{FWHM \cos \theta} \tag{3.2}$$

Where λ is the X-ray wavelength and θ is the diffraction angle.

3.7.2 Scanning Electron Microscopy (SEM)

Scanning electron microscopy (SEM) is a technique for high-resolution imaging. SEM is an electron microscope that use the electron in the primary beam is transmitted though the sample; both photon and electron signal are emitted as shown in Fig. 3.5. These signals include Backscattered Electrons (BSE), Secondary Electrons (SEI), Auger Electrons, Cathodoluminescence, X-rays, and heat. However, the electron signal that produces the principal means of viewing images in the SEM is secondary electrons which are given the topographical information of specimen surface. The difference in atomic number and in composition of specimen were using Backscattered Electrons detector [85]; the heavy elements (high atomic number) has a strongly backscattered electron signal than light element (low atomic number) which appeared brighter in image and showed the contrast between areas with different chemical composition. The energy dispersive x-ray spectroscopy (EDS or EDX) is the common accessory equipment which used to identify the element composition of a small specimen area.

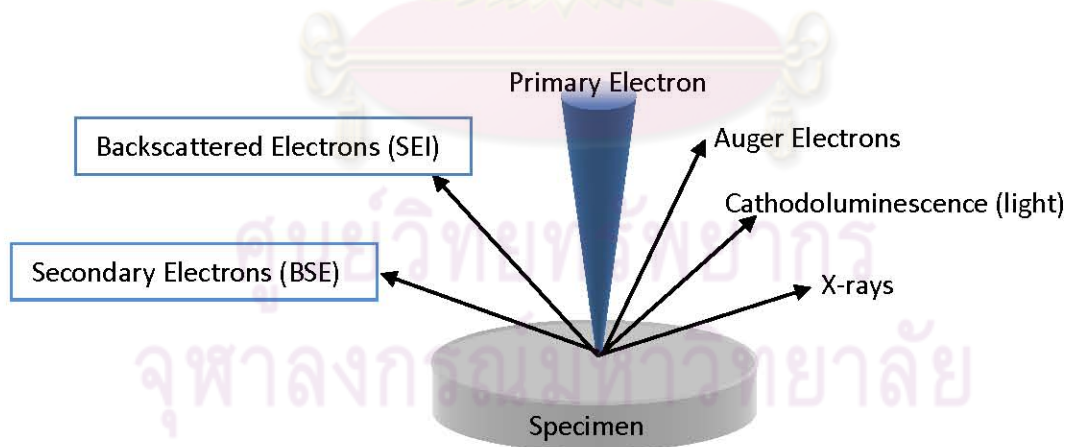


Figure 3.5: Schematic representation electron signals from the specimen.

3.7.3 Electron Probe Micro Analyzer (EPMA)

EPMA is also electron microscope like SEM and design for the non-destructive x-ray microanalysis and imaging solid material. The specimen was bombard with the primary electron beam. During the primary electron ionize the specimen atom, the inner shell electron were ejected, then the hole were replace by the higher- energy electron from an outer shell; the x-ray photon were release. As we know, every chemical element release x-ray with unique energy during the transferring process. Therefore, the emitting of x-ray by different energy can identify the type of sample atom. However, the resulting of x-ray spectrum can be reported according to energy and wavelength. The accessory equipment for each different detector is energy dispersive x-ray spectroscopy (EDS or EDX) and wavelength dispersive x-ray spectroscopy (WDS). In this work, WDS spectrometer of EPMA instrumentation [JXA-8100/8200 JEOL] was used. The WDS-analysis is suited for nitride sample because it can indentify light element with proper choice of crystal such as TAP (Thallium acid phthalate), PET (Pentaerythritol), LDE, LIF (Lithium fluoric) etc, which based on its ability to resolve peak and to exhibit high intensity peaks of an element [85]. Moreover, EPMA can use to measure the unknown specimen and obtain the quantitative analysis data by using ZAF method. In map analysis in EPMA, we can know the 2-dimensional distribution of elements on the specimen and the data is normally colored according to X-ray intensity (color map).

A schematic diagram of spectroscopy of X-ray by WDS is represented in Fig.3.6. A high energy electron beam is focused onto the sample; the x-ray was generated along with backscattered and secondary electron. Then, the intensity of isolated x-ray is quantified by an x-ray detector [86]. The wavelength of the sample from dispersion of x-ray is based on the diffraction of x-ray s that can explain by equation of Bragg's law.

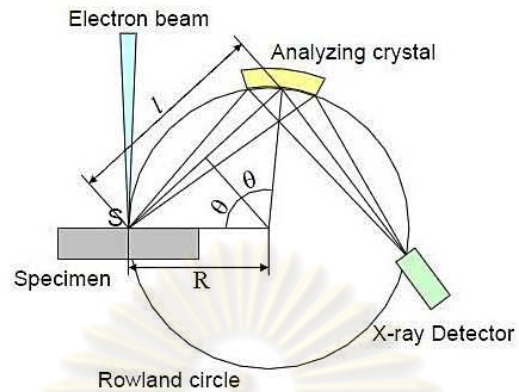


Figure 3.6: Spectroscopy by WDS [86]

3.7.4 Atomic Force Microscopy (AFM)

Scanning probe microscope (SPM) is a technique for obtaining topographical information of nanostructure surface [87]. Moreover, the film surface roughness and grain coarse processes can analyze by this technique. Scanning probe microscope can be divided into two types: scanning tunneling microscopy (STM) and atomic force microscopy. Both of techniques are different in case of resolution, type of material, and sample contacts. However, SPM is higher resolution than AFM but it is limited in conducting material. AFM- imaging modes consist of two modes: contact mode (CM) and tapping mode (TM). For contact mode, the tip on the AFM- cantilever scan on the surface sample with maintaining a constant force or constant height. In this work, tapping mode(TM) is used for AFM- imaging mode. In TM-AFM mode, the silicon tip placing on the cantilever is intermittent contact the surface of sample with an oscillation frequency circuit. The sample mounts on the piezoelectric scanner. Then, surface is scanned by a tip with the cantilever deflection.

3.7.5 Optical Microscopy (OM)

Basically, optical or light microscopy involves the light transmitted through sample or reflected from sample, then passing the single or multiple lenses for sample magnification and build up an image. The optical microscopy is a low cost tool which is used to analyze microstructure of sample in the range of 1-100 μm [88]. Moreover, optical microscopies mainly divide into two types: Reflected Light (RL) and Transmitted Light (TL). However, Transmitted Light (TL) is not suited for metal because of surface opaque. In RL microscopy is mostly used in material science because of good light reflection property which the sample must be polished before testing. For the light source, it requires the bright as possible which was created by various sources such as striking a carbon arc, resistance-heated carbon filament, and a xenon discharge tube. The brightness of light source with incidence on the half-silvered mirror was limited by condenser aperture. The condenser lenses focus the light onto the specimen which was magnified by objective lens.

In normal, the sample is tested using in Bright Field (BF) and Dark Field (DF) mode. The bright field illumination [89] only a proportion of the incident light is reflected or scattered back into the objective lens. In this mode, the polished surfaces appear bright, contrary, the rough area such as grain boundary show the dark [88] because of reflecting light from not go back to the object. In addition, Bright Field (BF) is usually in grain size measurement, and precipitates.

Dark Field (DF) is opposite the BF mode, the incident light is came up from an angle therefore polish area shows the dark and roughness surface show bright. Fig. 3.7 shows the diagram of light scattering of DF and BF mode.

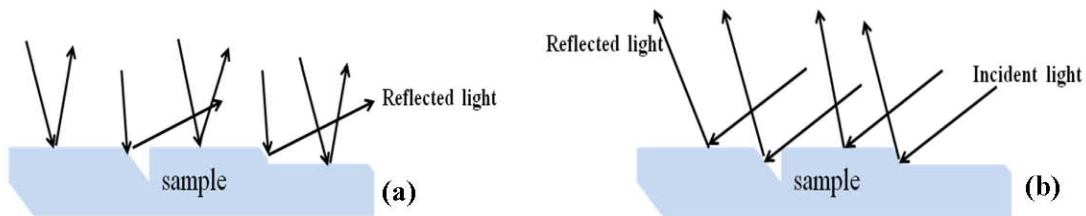


Figure 3.7: The diagram of light in DF (a), and BF (b) mode.

3.8 Plasma diagnostic

Plasma diagnostic is carried out by Optical emission spectra (OES) that is used to evaluate the emission intensity of the plasma species in plasma nitriding process including N_2^+ , N^+ , NH_x^+ , N,H_α , and H_β . This OES probe was placed on the top of chamber at a distance 10 cm from the quartz plate. The basic background of this equipment is based on the principles of quantum physics which established by Planck and Einstein. During glow discharge, the plasma process including dissociation, excitation of molecular vibration [59] and rotation are emitted the electromagnetic radiation (consist of photon) which is related to their wavelength corresponding with Planck and Einstein equation ($E = hf = \frac{hc}{\lambda}$). Emission spectrum is rescored the plasma species in term of wavelength(x axis) and mission intensity(y axis) that can use to explain ion density at different composition of gas mixture.

3.9 Techniques for Mechanical properties

3.9.1 Vickers Hardness Test

The Vicker hardness testing machine is very useful for testing microhardness of metal both soft and hard steels. This machine consists of the diamond indenter with the shape of square-based pyramid with an apex angle of 136° [89]. The test measure resistance to penetration and report the hardness by Vicker hardness number (HV) which calculate by the pyramid area of impression from the following formula [90]:

$$HV = \frac{2P \sin \alpha / 2}{d^2} = \frac{1.8544 \times P}{d^2} \quad (3.3)$$

Where HV = Vickers hardness in kg/mm^2

P = Load in kg

d = Average diagonal length of the impression in mm $[(d_1 + d_2)/2]$

α = Angle between the opposite faces of the pyramid ($\alpha = 136^\circ$ C)

3.9.2 Nanoindentation

Nanoindentation is a technique to measure the mechanical properties of material including elastic modulus (E_r), hardness(H), elastic recovery(R), contact stiffness (S) and deformation energies[91] in nano-scale range. Moreover, the wear resistant of coating films can be explained in term of mechanical properties including R, hardness-to-elastic modulus ratio (H/E_r), and elastic deformation energy (W_c) which obtained from nanoindentation tester [91]. Basically, this technique is base on a material resistance to permanent plastic deformation with similar micro hardness test [92]. The hardness data was reported after applied a load to indenter to force the tip press into the specimen surface. The measurer can set up the force or

penetration depth into the specimen with has a limit in the range 100 μm . After the indenter move out from the surface, then the specimen hardness was calculate from the load-depth penetration curve from Oliver and Pharr equation [93]:

$$H = \frac{P_{\max}}{A_c} \quad (3.4)$$

Where P_{\max} is the maximum indentation load and A_c is the projected contact area of indentation which depends on the indenter type.



ศูนย์วิจัยทรัพยากร
จุฬาลงกรณ์มหาวิทยาลัย

CHAPTER IV

CHARACTERISATION OF ALUMINIUM ALLOYS

4.1 Chapter review

From literature review (Chapter 2), has show that plasma nitriding of aluminium alloy has been achieved by DC source at high temperature. Moreover, the removal of aluminium oxide can be used the argon or argon-hydrogen gas mixture. The conditions for pre-sputtering must choose carefully, because Al_2O_3 prevent the diffusion of nitrogen into the alloy sample. Argon –hydrogen sputtering are suggested for plasma nitriding of aluminium alloy because of decreasing surface roughness on nitrided aluminium alloy surface. Generally, the successful to achieve a nitride layer by plasma nitriding has been published using DC source, and treated at longer treatment time. However, rf plasma nitriding is advantage for aluminium alloy because of high plasma density compared to DC source, which can lead to lower treatment temperature and shorter treatment time. Nitrogen is a carrier gas for nitriding, which is mostly used in both of DC and rf source. In addition, some of researchers are also used hydrogen-nitrogen for nitriding process. Most of researchers have been believe that addition hydrogen can lead to achieve the nitrided layer. However, some reviews are reported about insignificant hydrogen addition during nitriding process. Moreover, no publication about hydrogen mixture in plasma nitriding for rf plasma nitriding of aluminium alloy was reported.

Characterization of nitrided aluminium using X-Ray diffraction pattern can confirm the forming of AlN hexagonal AlN-phase. Moreover, AlN (100) plane is often observed after treatment aluminium alloy, which is highest intensity peak of an AlN powder standard. The main aim of this work describes in this chapter was characterization of nitrided aluminium

alloy formed on aluminium alloy surface under low treatment temperature and treatment time using XRD, and EPMA. The influence of hydrogen addition for forming nitrided layer also described using XRD data.

4.2 Material investigated

In this work, aluminium 2011 was chose for rf plasma nitriding because of its commercially availability. The aluminium alloys 2011 consist of majority element of copper and small amount of various elements including Si, Fe, Pb, Bi, Zn and so on. Therefore, as part of investigation the effect of hydrogen in plasma nitriding process, we changed the nitriding material to Al-6wt%Cu to avoid the effect of composition of material during plasma nitriding process. For al-6%wt sample is cast alloys in cylinder shape which mainly consist of aluminium and copper.

4.3 Influence of rf plasma nitriding edge effect of aluminium alloy

The edge effect was normal problem which was found in DC plasma nitriding because of non-uniform plasma and distortion of electric field at edge area of sample [94, 95]. Moreover, recent studies by Kattareeya et al. [96] reported that, rf-ICP plasma nitriding of aluminium alloy can be created the edge effect which due to the higher sputtering at the edge of sample. From the experimental result, the edge effect also found in rf plasma nitriding of Al2011, but evidently did not see the ring around the corner of nitrided sample, as shown in Fig.4.1(c). It could be the without of nitride layer or thin nitrided layer was formed. However, the edge effect of sample can increase the concentration of nitrogen as shown in Fig. 4.2. The atomic% of nitrogen at the edge zone is higher than interface and center zone because at the edge of sample has high current density which causes high sputtering and induce the implantation of nitrogen into surface of sample.



Figure 4.1: Surface morphology of a) Untreated sample, b) After pre-sputtering with Ar-H₂ for 1 h, and c) After nitriding with N₂- H₂ for 25 h

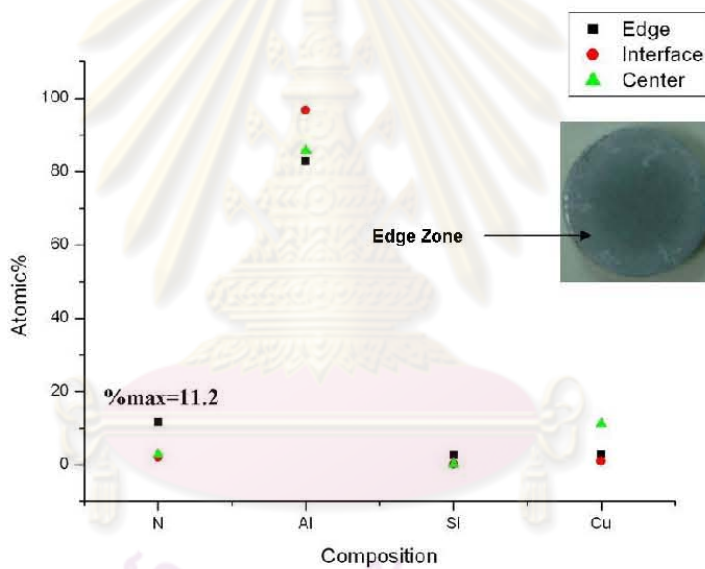


Figure 4.2: The atomic% of element including N, Al, Si and Cu at three zones (edge, interface and center) of nitrided sample for 25 h.

4.4 Effect of sputtering in plasma nitriding of aluminium alloy

Normally, a thin aluminium oxide (Al_2O_3) exists on the surface of aluminum material [14] which is barrier the nitrogen diffusion of nitrogen into the aluminium alloy surface. The elimination of Al_2O_3 has been used sputtering process with argon gas or argon-hydrogen gas mixture. However, both of pure Ar sputtering and Ar- H_2 sputtering indicated an increase in roughness after plasma nitriding for 25 h as shown in Fig.4.2. From figure, the average surface roughness (R_a) increased from 120.44 nm in untreated sample to 218.64 nm, and 199.49 nm in samples that were sputtered with pure Ar, and with mixed Ar- H_2 respectively. In fig. 4.1(b), after sputtering with Ar- H_2 , the color of surface changes to white color and non-uniform comparing to untreated sample (Fig.4.1 (a)). Therefore, the aggressive sputtering causes the surface damage and increasing roughness in nitrided sample.

Sputtering of aluminium alloy can result in high surface roughness because alloying element alloy and native oxide in aluminium alloy have different sputtering yields. When sputtering with Ar, the aluminium atom can eject from aluminium alloy easily than oxide because high sputtering yield compared with the sputtering yield of Al_2O_3 [60]. Therefore, long pre-sputtering is required to complete for oxide elimination which cause the surface roughness on sample. However, the surface roughness from Fig. 4.2 (c) slightly decreases with the addition of H_2 in pre-sputtering process. Because of addition hydrogen under constant total sputtering pressure can reduces the sputtering rate of Ar. Hydrogen has a small mass which cause a lower sputtering yield, and lead to reduction in the concentration of ionize Ar [97]. The energy from plasma source was used to dissociate molecular hydrogen atom and transfer energy for first ionization potential of hydrogen and argon atom (≈ 13.6 eV, and 15.8 respectively).

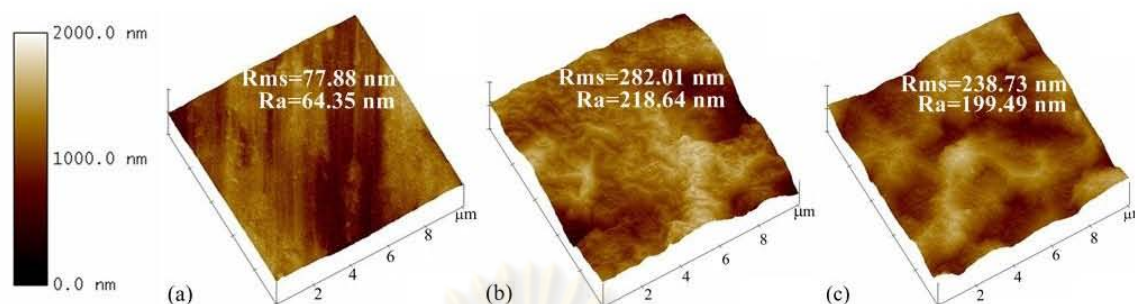


Figure 4.3: 3D AFM images of 10 μm x 10 μm sample surface sputtered with different gas as (a) untreated, (b) Ar-sputtering, and (c) Ar-H₂ sputtering samples.

From OES observation, the intensity of Ar⁺ peak of argon sputtering is higher than Ar⁺ in Ar-H₂ sputtering, as shown in Fig. 4.4. During pre-sputtering process, argon atoms do not need the addition energy to form atomic argon species because they are a single atom form. However, shorter time of sputtering is not significant decreased surface roughness by using argon-hydrogen gas mixture as shown in Fig.4.2. Because, the Ra value of argon sputtering and argon-hydrogen is similar. We conclude that Ar-H₂ tend to decrease the surface roughness because it decreased the number of Ar⁺ for ions surface bombardment.

ศูนย์วิจัยทรัพยากร
จุฬาลงกรณ์มหาวิทยาลัย

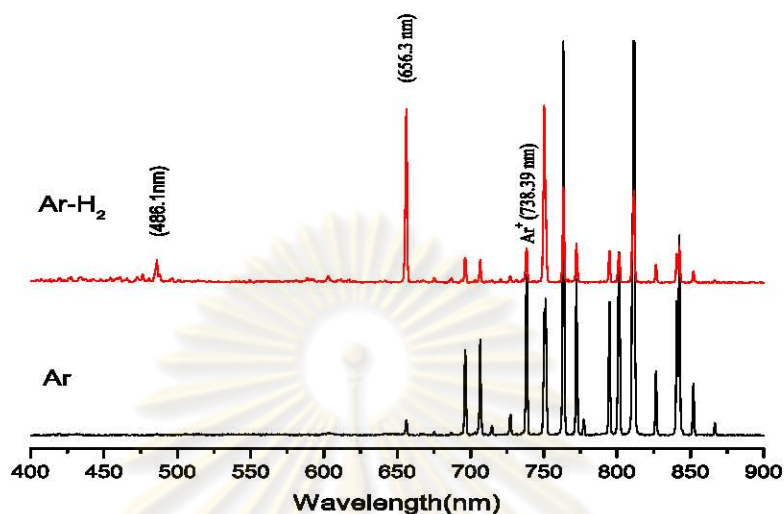


Figure 4.4 Emission spectra of Ar and Ar-H₂ mixture at 1 torr in wavelength of 450 nm to 900 nm

4.5 Effect of treatment time

4.5.1 Experiment, results and discussions

In this part, aluminium alloy 2011 was used in plasma nitriding at different treatment time (9 h, 16 h, 25 h, and 36 h). The aluminium oxide layer was eliminated with the ions bombardment of Ar-H₂ gas admixture at pressure 1 torr, and the rf power was fixed at 100 W for 1 h. Both of pre-sputtering and nitriding process was evacuated by rotary pump and diffusion pump up the base pressure to 5.5×10^{-5} torr. For heating the specimen during nitriding process, the halogen bulb which placed under the substrate holder was used at working temperature 350°C. The admixture of N₂ and H₂ gas was introduced in the chamber with ratio 1: 3 for plasma nitriding process and the rf power was set between 100 - 300 W while the different substrate bias voltage from -100 to -400 V were applied. In the present study, the long treatment time is clearly effect the surface roughness, as shown in

Fig. 4.5. Moreover, from SEM observation of different nitriding times of (a) 9h, (b) 16 h, and (d) 25 h, the damaged surface layer was clearly observed at treatment time of 16h, and 25 h, as shown in Fig.4.5. When the treatment time is longer, the roughness was high because the ion sputter including N_2^+ was continuously sputtered to the surface. Therefore, the roughness of nitrided surface is strongly dependant on the increasing nitriding time.

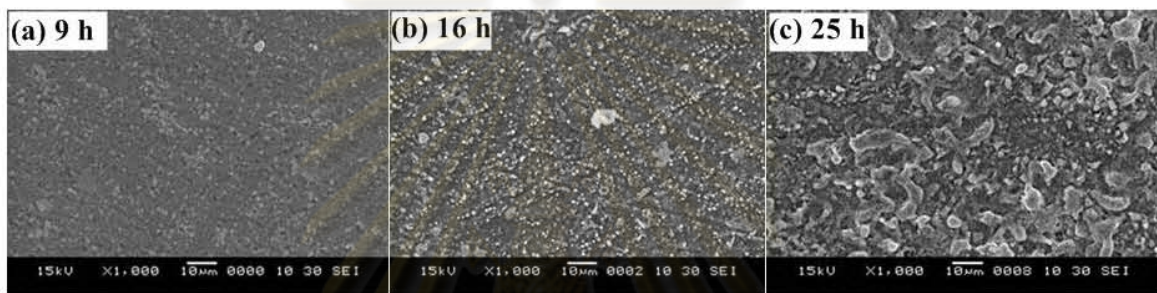


Figure 4.5: SEM image of samples treated with nitriding process for (a) 9 hr, (b) 16 hr and (c) 25 hr

To study the influence of the plasma processing time on the nitrogen composition in nitrided aluminium alloy, EPMA/WDS was measured. Mapping images of nitrogen and aluminium at nitriding time 9 h, and 16 h show in Fig. 4.6. The color scale bars were used to estimate the distribution of elemental on nitrided surface. The pink color and black color represent the high and low each element distribution respectively. At treatment time for 16 h, the dots of the light blue color (nitrogen mapping) become bigger when compare with nitriding time 9 h. The observation of light blue color is clearly evident that the nitrogen concentration in the nitride layer increase, which implied that the AlN volume fraction also increases. Moreover, in the aluminium mapping for nitriding time 16 h, green color dots speared more than that of nitriding time of 9 h. The aluminium elemental on the surface was replaced with other element as long treatment time.

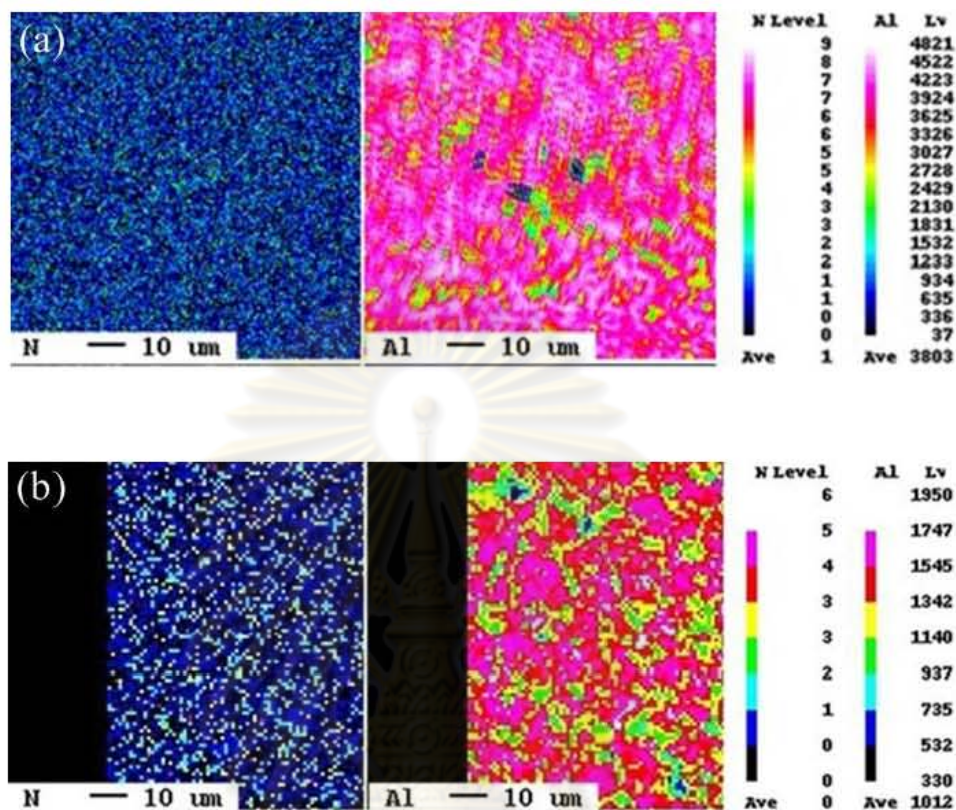


Figure 4.6: Nitrogen and aluminium maps showing the distribution of nitrated surface at different nitriding time (a) 9 h; and (b) 16 h. The colored scale bar show the comparative concentration condition at 10 μm step size.

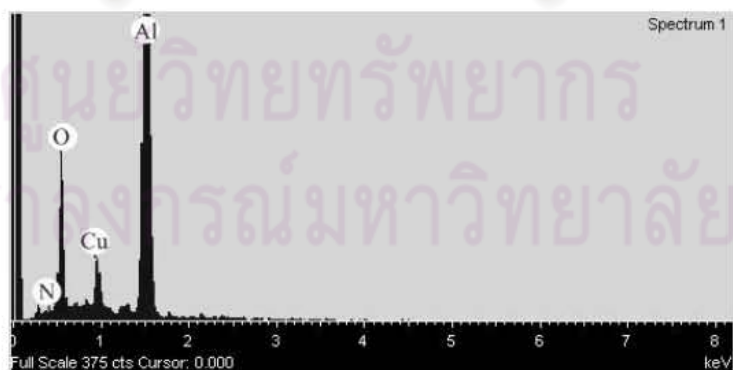


Figure 4.7: EDX analysis of nitrided Al₂₀₁₁ for 25 h

The GIXD pattern of the plasma nitrided Al2011 is shown in Fig. 4.8. At treatment times of 25 h, the aluminium nitride (AlN) and aluminium copper (CuAl_2) were formed. According to jcpds#01-075-1620(see appendix B), the existence phase present in the nitride layer is hexagonal AlN (lattice parameters $a = 3.11 \text{ nm}$ and $c = 4.98 \text{ nm}$). In addition, the diffraction peaks of AlN at $2\theta = 33.20^\circ$ can be clearly observed, but small peaks. The (101) orientation of AlN and (211) of CuAl_2 are located at the same position ($2\theta = 37.91^\circ$), therefore we cannot confirmed the AlN(101) was formed. From figure 4.8, diffraction spectra from the Al and CuAl_2 were observed at higher position than the peak of AlN, indicating that amount of AlN formed on the surface is very small. The small peaks of AlN can explain in many reasons: first, this experiment work as high pressure which causes the oxide can easily to re-form on specimen again. Second, referring to Gibb energy, copper can combine with aluminium easily than nitrogen and then form small grain of CuAl_2 which prevent the nitrogen to diffuse into specimen. Nevertheless, AlN (100) shows strong intensity peak than other peak which can confirm the AlN formation.



ศูนย์วิทยทรัพยากร
จุฬาลงกรณ์มหาวิทยาลัย

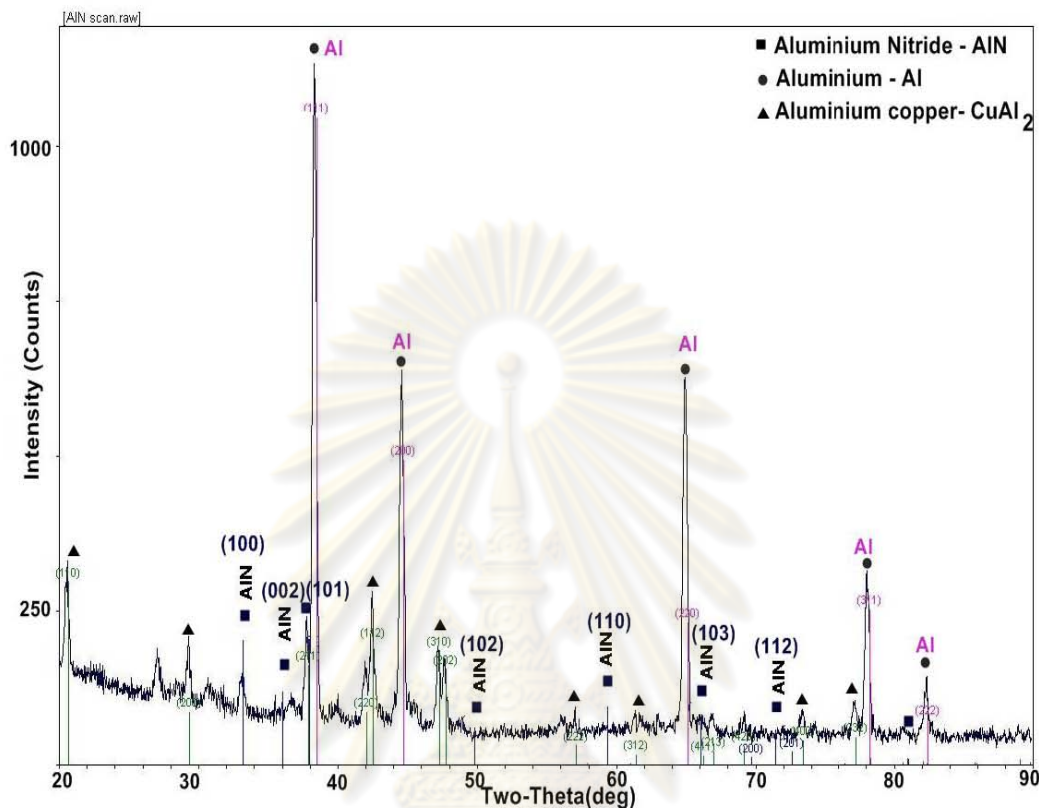


Figure 4.8: GIXD pattern of nitride Al 2011 at 250 V bias voltages, 400°C treatment temperature.

Because of the thin layer was formed in this experiment. Moreover, the high roughness was also observed as shown in Fig.4.3. Therefore, the mechanical properties of nitrided Al2011 cannot be measure with micro-hardness equipment. In this case, nanoindentation with cube-corner indenter was used to measure the hardness because of avoiding the tip effects in nanoindenter. From the result of hardness, there were only minimal changes of hardness after plasma nitiding in most of the samples, for instant, in sampled treated for 25 hour the hardness was increased from 259 HV to 270 HV at a maximum force of 1000 μ N. Taweesub et al. [96] reported the hardness measurements using AFM indenter increase from 405 HV to 1740 HV after if nitriding of Al-6wt%Cu for 25 h which higher than the nitrided layer from

Vickers hardness measurement. In this experiment, the nitrided aluminium alloy cannot increase the surface hardness compared to Taweesub [96] may be due to the different in surface roughness in untreated and treated which cause to achieve the nitride layer on the aluminium alloy surface.

4.5.2 Summary

Increasing nitriding time from 9 h to 36 h did not significantly increase the nitrogen concentration in the nitrided layer and produced a deeper case depth. However, using XRD we can indicate that the AlN was formed with increasing nitriding time at least 9 h. Moreover, it can be clearly seen that the surface roughness increased significantly as a function of nitriding time. Because of very thin layer was formed on nitrided of Al 2011, therefore hardness and thickness cannot be characterized. Therefore, we can summarize that if plasma nitriding cannot improve the surface hardness and archived the nitrided layer of Al2011.

4.6 The effect of hydrogen in rf plasma nitrided aluminium alloy

4.6.1 Experiment, results and discussions

In this part, Cast Al-6wt%Cu alloy was used as a material to be nitrided. In addition, the effect of the percentage of addition hydrogen in plasma nitriding was investigated. The cast Al-6wt%Cu sample consist of a few elements when compare with Al2011, and avoid the effect of alloying elements in aluminum alloy in plasma nitriding process, therefore cast Al-6wt%Cu was chosen. The base pressures were also same as in plasma nitriding of Al2011 (5.5×10^{-5} torr). But we changed the high vacuum pump from diffusion pump to turbo molecular pump to avoid the oil contamination. For pre-sputtering process, the Ar-H₂ gas

mixtures was also used, but decrease the working pressure to 0.5 torr at 0.5 h. For nitriding process, the nitriding time was set for 6 h. The temperature was controlled in a range 290-316 °C in order to prevent local melting of substrate. The substrate was DC biased at -300 V.

As claimed by other researchers, adding hydrogen in plasma nitriding, can be used for surface modification of Aluminium alloy and steel [4, 12]. In nitriding process, the effect of hydrogen in N_2-H_2 was also reviewed in chapter 2. At gas mixtures of nitrogen-hydrogen atmosphere, it is significant enhanced to form the nitride layer in nitriding process. Most of studies are investigated on plasma nitriding of steel, aluminium in DC plasma. Only few studies have been carried out with N_2-H_2 discharge for plasma nitriding of Al by rf-ICP. Moreover, the available literature did not report on the effect of N_2-H_2 gas mixtures on rf-ICP plasma of aluminium alloy. When we observed by OES we found that lines of N_2^+ (391.44, 427.8 nm), β H Balmer (486.13 nm), were detected in the emission spectra. Moreover, the NH (336 nm) line was also observed. It was reported that this NH specie play an important role for the nucleation and growth of nitride layer. Nevertheless, the increasing ratio of $N_2:H_2$ did not obviously affect the distribution of species in plasma (in fig.4.17). It can be seen that the emissions of plasma species are similar for all spectra even with different $H_2:N_2$ ratio variation as 1:1, 2:1, and 1:2. Therefore, optical emission spectroscopy could not be used to investigate the effect of different ratio of $N_2:H_2$. In this work is corresponded with Czerwiec [83] that the emission spectra at different $H_2:N_2$ ratio cannot be distinguished by OES spectrometry under low pressure condition. However, it was useful for investigation of NH species which occur during nitriding process. In this work, the H_2-N_2 gas mixture was used as a plasma gas, which was varied with various ratio including 25 H_2 %+75 N_2 %, 50 H_2 %+50 N_2 %, 75 H_2 %+25 N_2 %, and pure N_2 under a chamber pressure of 0.4 torr, at an rf power of 200 W for 6 h.

From Fig.4.9- 4.12 show the EPMA/BSE micrograph after nitriding with 25% H_2 , 50% H_2 , 75% H_2 and pure N_2 , respectively. The big white spots can be seen in Fig.4.9, which is due to the sputter effect. When increasing the hydrogen partial pressure is shown the small white spots and hole as shown in Fig.4.10 and Fig. 4.11. This is probably due to increasing hydrogen percentage is created more energetic ions which make a drastic ion bombardment. In pure nitrogen, the white dots are seemed to decrease the size and spread over the surface. Moreover, adding hydrogen with nitrogen plasma and pure nitrogen plasma during nitriding process are changed the samples color to gray-black color in the middle of sample with significantly asserted AlN on sample. Fig.4.12 is clearly exhibited the ring around the edge of sample, which is called the edge effect that is caused by the concentration of electric field lines of biased sample [98].



ศูนย์วิทยทรัพยากร
จุฬาลงกรณ์มหาวิทยาลัย

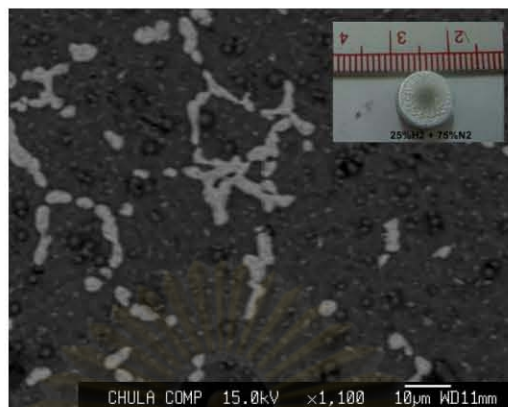


Figure 4.9: EPMA/BSE micrograph of Al-6wt%Cu after plasma nitriding in 25%H₂ of total gas pressure.

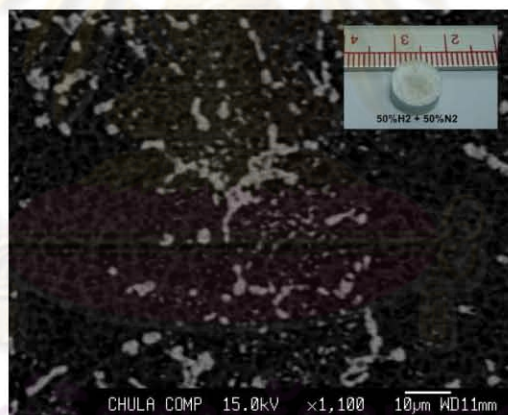


Figure 4.10: EPMA/BSE micrograph of Al-6wt%Cu after plasma nitriding in 50%H₂ of total gas pressure.

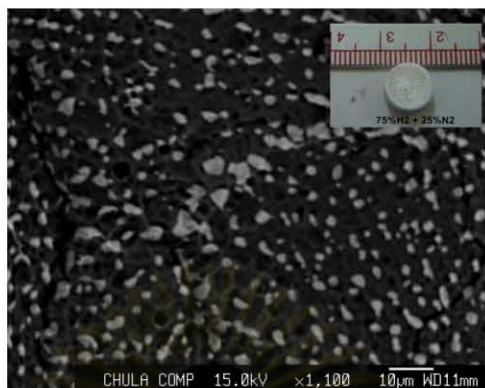


Figure 4.11: EPMA/BSE micrograph of Al-6wt%Cu after plasma nitriding in 75%H₂ of total gas pressure.

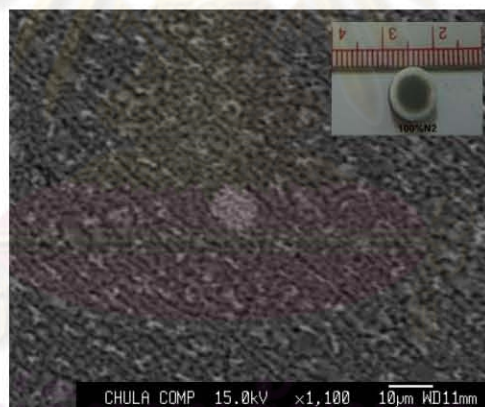


Figure 4.12: EPMA/BSE micrograph of Al-6wt%Cu after plasma nitriding in pure nitrogen of total gas pressure.

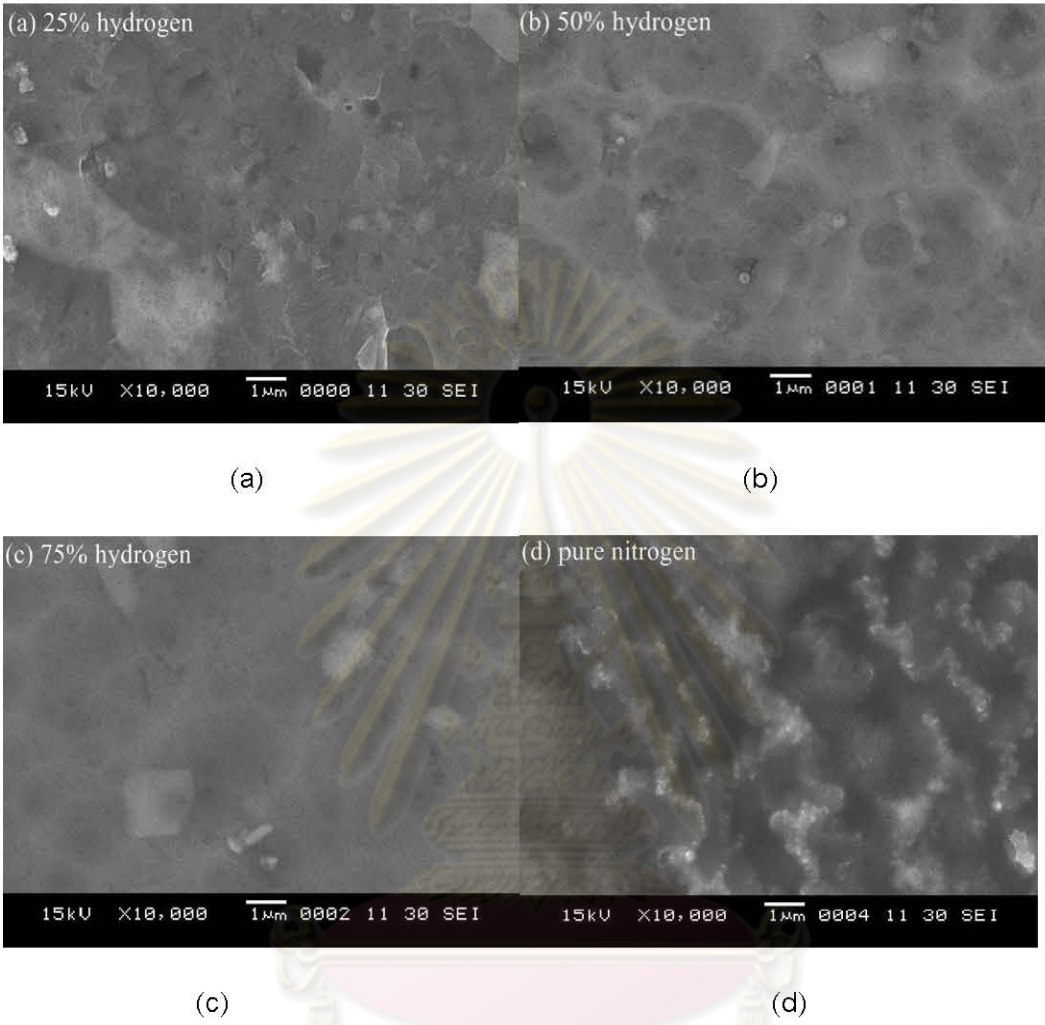


Figure 4.13: SEM micrograph of Al-6wt%Cu after plasma nitriding in different gas mixture; (a) 25% H₂; (b) 50 % H₂; (c) 75 % H₂ (d) Pure Nitrogen

Fig.4.14 illustrates the white pattern on nitrided surface at 250 W. By EPMA mapping, the white pattern show pink color which means rich copper in this area.

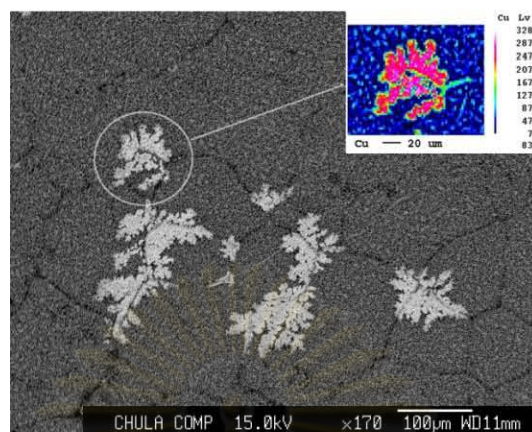


Figure 4.14: The EPMA mapping of plasma nitriding, pure nitrogen, at 250 W.

As the result, plasma nitriding 25% H_2 and 75% N_2 has a higher surface roughness compared to that treated with pure-nitrogen. This is probably due to the fact that it was sputtered by hydrogen plasma. K.S. Suraj *et al.* [95] conclude that additional hydrogen increases the tail of the electron energy distribution function (EEDF), which raises the electron temperature. Additionally, it is also increased the ionization rate and the plasma density which is raised the energetic ion to bombardment the sample. Moreover, qualitative analysis with WDS-EPMA indicated the atomic % of nitrogen, copper, aluminium, and magnesium with various spectrometers containing several analysis crystals including LDE, LIFH, and TAP, respectively, which is different in the interplanar spacing of the reflecting plane (d) for each crystal [99]. By using EPMA-mapping, the amount of nitrogen was distributed over the sample; nevertheless, it's not evidently confirmed forming AlN on substrate, because the phase between aluminium and nitrogen is indistinctly observed on mapping. However, the results of all samples are surely confirmed the forming AlN because of the resulting XRD pattern.

Fig.4.15 is shown the x-ray diffraction spectrum of rf plasma nitriding treated at different H₂ ratios. It can be seen that the most peak are observed in Al, CuAl₂, and AlN phases. However, the patterns indicate that the main phase on the surface after plasma nitriding is CuAl₂ which form the compound layer that cover entire surface to correspond with the EPMA results. Besides, the XRD results also show a wurtzite AlN according JCPDS number 075-1620 (see Appendix B) formed on the top surface of the specimen. The AlN peaks are identified for (002), and (101) planes. It can be seen that the intensity of AlN peaks are very low showing that amount of AlN formed on the surface is low. The amount of AlN formed in this experiment is low possibly due to relatively short processing time (6 h) and lower treatment temperature (range between 290 and 316 °C). However, among the addition hydrogen during nitriding process, the evident peak in (002) plane of AlN was shown hydrogen percentage at 50%, which agrees with Negm *et al.* [79]. Elsewhere, in (101) plane of AlN was exhibited only pure nitrogen in nitriding process. From XRD result, CuAl₂ is also detected due to the precipitation of CuAl₂ in the Al-6wt%Cu substrate. The particle size was estimated using Scherer formula $D = 0.9\lambda / \beta \cos \theta$, where λ is a wavelength of Cu K α radiation ($\lambda = 1.54 \text{ \AA}$), β full width at half of maximum (FWHM), and θ is the angle. Increasing the hydrogen ratio, the FWHM is also increased on the (200) plane of AlCu₂; an estimate of the grain sizes at 25% H₂, 50% H₂, 75% H₂ and pure nitrogen are shown 34.97 nm, 35.29 nm, 24.00 nm, and 26.74 nm, respectively. Therefore, it is indicated that the grain sizes are decreased due to the increasing percentage of hydrogen. Using FWHM of (200) plane, the crystal size of AlN was calculated to 19.50 nm for the addition 50% of hydrogen in the gas mixture. Furthermore, using pure nitrogen plasma is estimated the size to 41.00 nm.

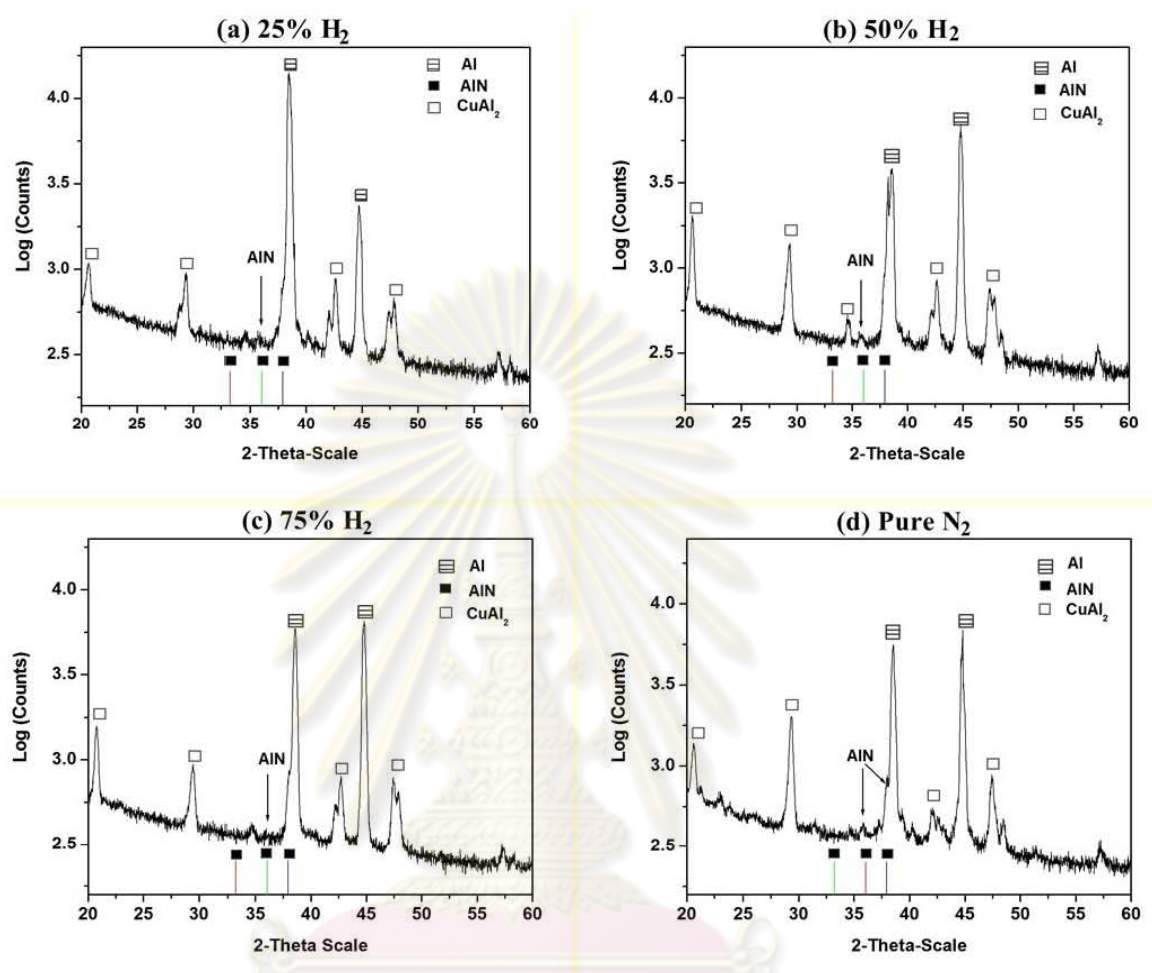


Figure 4.15: X-ray diffraction pattern of Al-6wt%Cu if plasma nitriding at 200 W for 6 h, as various hydrogen percentages (a) 25%H₂, (b) 50%H₂, (c) 75% H₂ and (d) pure N₂

Fig. 4.16 is shown the emission intensity of pure N₂ and 25% H₂ in the gas composition during nitriding process. Both the two lines are same except at the wavelength lower 500 nm. At these conditions, it can be implied that adding hydrogen does not decrease the emission intensity of nitrogen discharge, but create a new species such as NH_x⁺ which affect to the plasma nitrided surface [40].

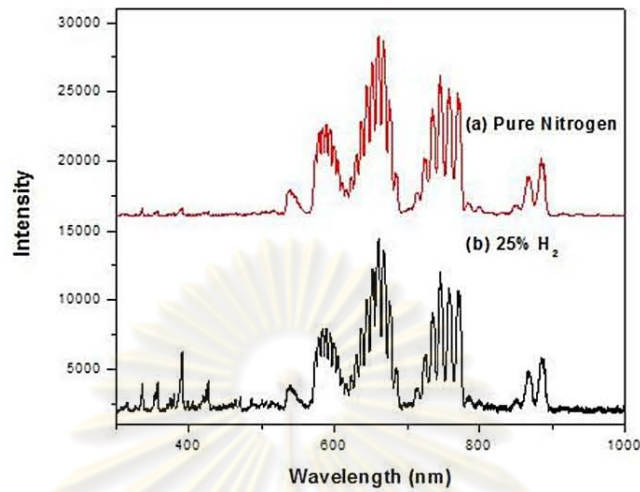


Figure 4.16: Emission spectra of N_2 - H_2 mixture at 0.5 torr in wavelength of 300 nm – 800 nm

The estimation of hardness is observed using nanoindentation with Berkovich diamond indenter. This instrument was used to measure some condition including untreated sample, treated sample (25% H_2 , pure nitrogen), because it was limited by roughness of sample. The average hardness of treated samples including 25% H_2 , and pure nitrogen are shown the result 1.9350 GPa, and 2.3451 GPa, respectively. The data of treated sample is exhibited a bit increasing hardness to compare with untreated sample (1.1206 GPa). Moreover, the graph of loading during nanoindentation measurement is shown an unsmooth curve; because of the porous film that it make the calculation hardness lower than the real data. In this work, the high roughness surface is extremely observed. The affect of high roughness is considerably in hardness test result using nanoindentation, which is in agreement with Jian *et al.* [100].

4.7 Effect of rf power

Figure 4.17(b) shows the nitrided of sample after nitriding of Al-6wt%Cu at 250 W for 6 h. From this figure, the treated sample at 250 W is uniform color than treated sample at 200 W (Fig. 4.17a). The resulting of increasing the rf power is the high degree of ionization which can increase the plasma density. Therefore, the large species can react with the sample which causes the changing color.

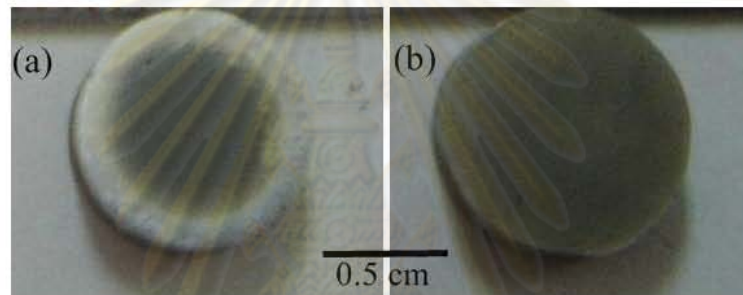


Figure 4.17: Al-6wt%Cu plasma nitriding with pure nitrogen at different rf power (a) 200 W (b) 250W

4.7.1 Summary

From the rf Plasma of pure nitrogen or N_2-H_2 mixture in nitriding process by using RF plasma generator with rf power of 200 W with substrate biasing of 300V DC for 6 h can be performed Wurtzite-type AlN. Increasing amount of nitrogen significantly affects morphology of nitrided specimens which indicates its effect on formation of AlN. However, amount of AlN formed by rf plasma nitriding is very low after 6 hour nitriding, then, no significant different amount of nitrogen can be detected by WDS. Therefore, we can conclude that the different element in aluminum alloy and with and without hydrogen addition cannot significant for forming AlN on aluminium alloy surface.

CHAPTER V

CHARACTERISATION OF THE NITRIDED LAYERS OF AISI H13 STEEL

5.1 Chapter review

As shown in chapter 4, nitride layer on Al alloy using rf-ICP has been formed at low temperature, but relatively thin nitrided layer and high surface roughness were observed. However, in the case of the nitriding of H13 experiments, the nitrided layer was easily formed on the H13 surface compared to aluminium due to the oxide on surface not barrier the nitrogen diffusion into the surface. Generally, increasing case depth of nitrided layer mainly depends on increasing of two parameters; long treatment time and high temperature. Unfortunately, working metal at high temperature can change the properties of bulk material. Therefore, many researchers have tried to achieve the deeper case depth of nitrided layer at low temperature. Therefore, the aim of this chapter, plasma nitriding of H13 steel using rf-ICP at low treatment temperature, is presented.

ศูนย์วิจัยทรัพยากร
จุฬาลงกรณ์มหาวิทยาลัย

5.2 Effect of sample

In the first part of nitriding of H13, the AISI H13 of 2 mm thick was used in rf plasma nitriding at 0.5 torr fixed pressure with 50% H_2 -50% N_2 gas mixture for various nitriding time (1h, 9h, and 12h). We found that a few color change after nitriding time of 1 h and 9 h, as shown in Fig. 5.1a and 5.1b. The main reason is because of the effect of workpiece geometry between substrate holder and quartz plate which is the one of parameter affect to achieve nitride layer. However, the color of surface sample changed from metallic to gold color and exhibited ring around the edge of sample (in Fig.5.1c) because abundant of charge density [96]. To summarize the results of 2 mm thick plasma nitriding, we can conclude that the height of sample and treatment time affect to achieve nitride surface because black color is not forming. Therefore, the size of sample was changed as shown in Fig. 5.2.



Figure 5.1: The comparison of surface color after nitriding of: (a) 1h, (b) 9 h, (c) 12 h.

5.3 Effect of treatment time

5.3.1 Experiment, Results and discussions

In the pretreatment process, plasma of argon, and hydrogen mixtures were used to clean sample surface for 20 minutes, with rf power 80 W under chamber pressure of 1.2 torr. A molecular turbo pump was used to evacuate to the base pressure. The hydrogen and nitrogen gas were introduced into the chamber to the total pressure of 0.5 torr with pressure ratio of 1:1. During the nitriding process, the sample was heated up to 300°C. H13 samples were plasma nitrided for 1, 4, 9, 12, and 20 hours using 100 W rf power. The negative bias of 300 voltages was also applied to the sample to attract ion to sample surface.

After rf plasma nitriding, color of Plasma nitrided H13 is different from the untreated sample, as shown in Fig.5.1. It can be clearly seen that the surface of nitrided H13 sample appeared in dissimilar color after nitriding for 20 hours comparing to the untreated sample of shiny metallic color. After nitriding, a non-uniform color in the entire surface of the sample is observed. The color at the edge of sample is black and become brown color at the center of sample. This is probably due to the fact that the non-uniform of plasma with depends on shape of plasma sheath and shape of sample which cause effect to ion flux distribution. Normally, the edge effect mostly has been found in DC plasma nitriding at the edge of sample. Nevertheless, in previous chapter, we found that the edge effect also occurred in nitriding of aluminium alloys. Therefore, we can summarize that the edge effect can be occur both of aluminium alloy and H13 which is strongly depended on plasma properly cause the non-uniform sputtering. As it well known, rf source can be generated uniform plasma than DC source. The explanation in this case is that the sample was biased which also cause edge ring. Therefore, low bias voltage or without bias voltage tend to decrease the edge effect in nitrided sample with rf nitriding. Ahangarani et al. [101] suggest that active screen plasma nitridin can used to decrease the

edge effect as nitriding process. From experiment result, we found that the ring edge of nitrided sample can be clearly seen when the nitrided layer is thick (comparing between nitrided aluminium alloy and nitrided H13).

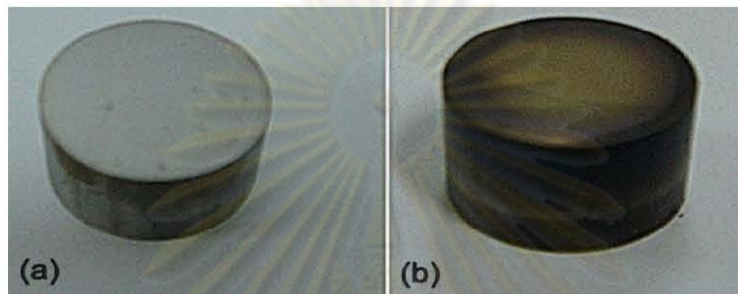


Figure 5.2: Appearance of AISI H13 samples (a) untreated, and (b) treated.

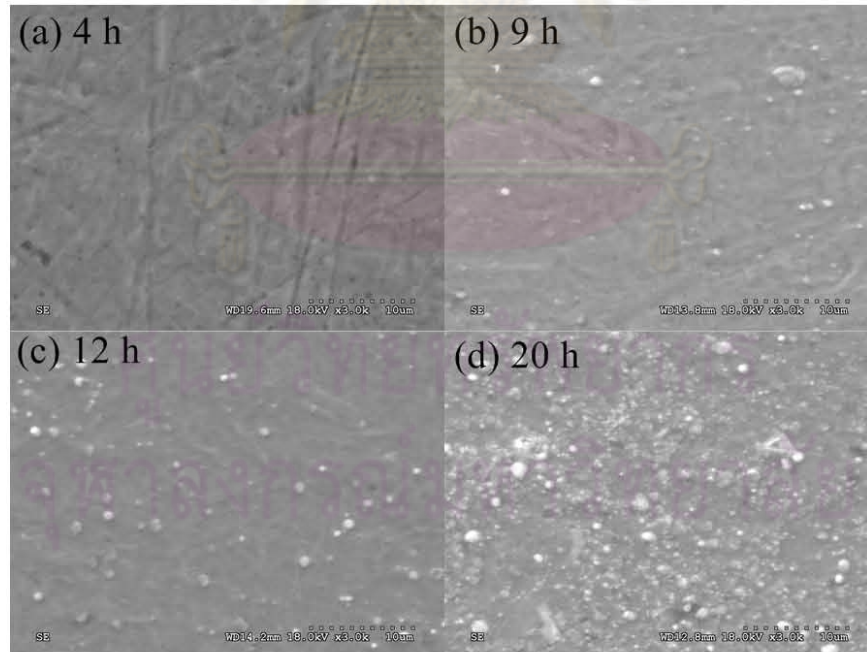


Figure 5.3 : SEM micrographs of a AISI H13 surface treated at different time; (a)4 h, (b) 9h, (c)12 h, and (d) 20h.

The influence of increasing treatment time is clearly seen with the morphology and roughness of nitrided sample as shown in Fig. 5.3 and Fig.5.4, respectively. From Fig. 5.3, the white spots were observed over the sample as nitriding for 20 h, with corresponding to the increasing roughness in nitrided sample in Fig.5.4. From the AFM results, the average roughness of the surface before nitriding was 5.8 nm. After nitriding, the surface roughness increase to 27.61 nm and 36.0 nm for nitriding time of 9, and 12 hours, respectively. The surface roughening after plasma nitriding is unavoidable [12, 27] because the sputtering process during nitriding process is continuous working. Hence, the increasing of the nitriding time affects on increasing the surface roughness.



ศูนย์วิจัยทรัพยากร
จุฬาลงกรณ์มหาวิทยาลัย

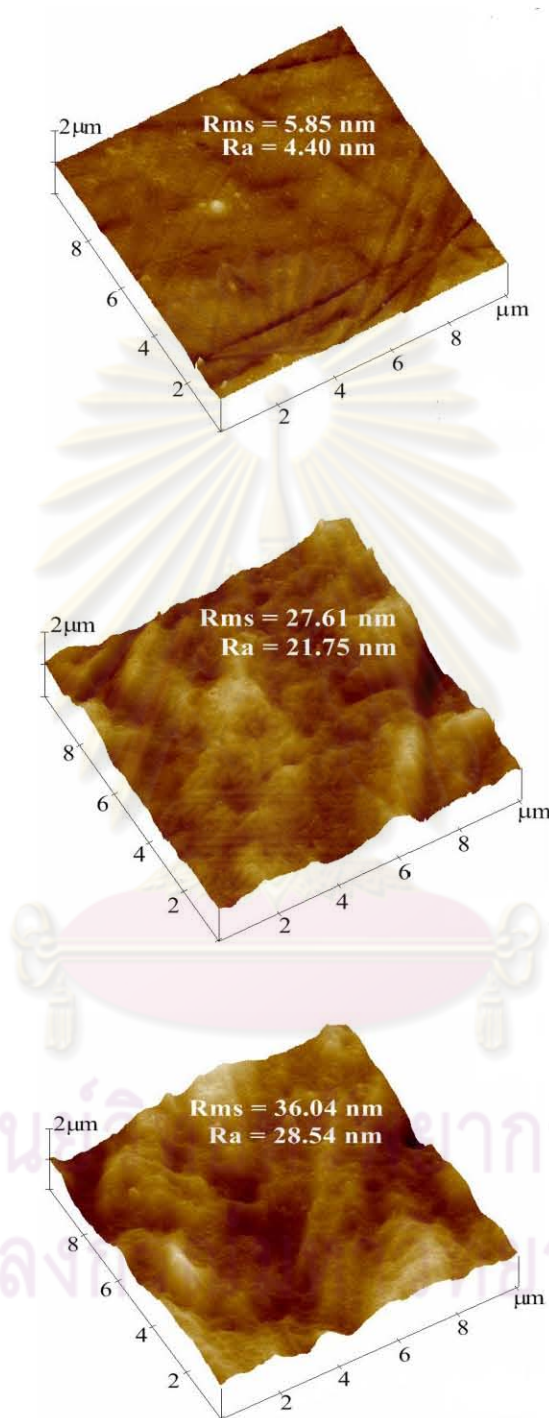


Figure 5.4: AFM images with nitriding time of: (a) untreated, (b) 9 h, (c) 12 h

In order to obtain the cross sectional of the nitride sample must be prepare in following step: cutting by diamond saw, and cleaning. The sample was mounted in phenol formaldehyde or Bakelite. Then, the mount sample was polished by silicon carbide polishing paper. For electron microscope testing, the mount sample was etched with 1-2% natal for showing the thickness of sample.

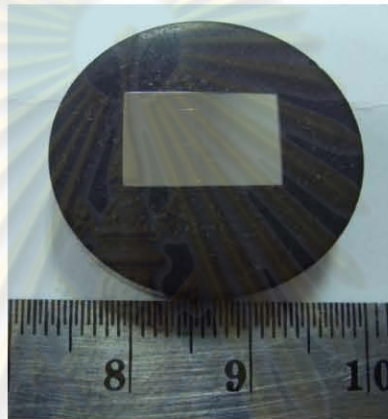


Figure 5.5: The mount sample (12 h nitriding) for cross sectional testing

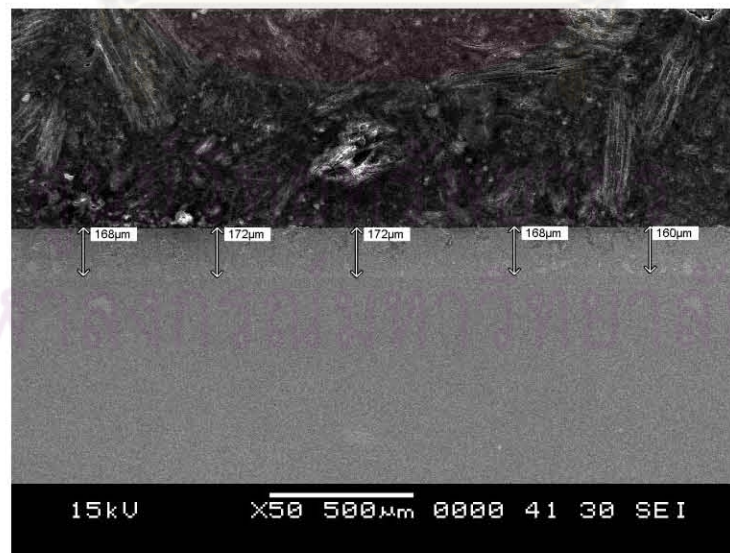


Figure 5.6: SEM cross section of AISI H13 nitriding for 20 h.

The nitride layer with thickness up to 150 μm can be seen by OM and SEM (Fig.5.6 and Fig.5.7, respectively). According to the OM microstructure the nitrided layer by rf plasma nitriding shows only the nitrided layer with precipitate of nitride particles and solid solution of nitrogen atom without the compound layer formation on the top surface. The average thickness of nitrided layer increases from 12.6 μm to 157.6 μm with increasing nitriding time from 9 to 20 hours as shown in Fig. 5.7.

As shown in Fig.5.8, the scattered electron (BSE) images in SEM shows the thick of the edge sample for the 20 h nitrided specimen. It can be seen from this figure that diffusion layer can appear not only the top of sample but also lateral area which is relate to black color as shown in Fig. 5.1(b).

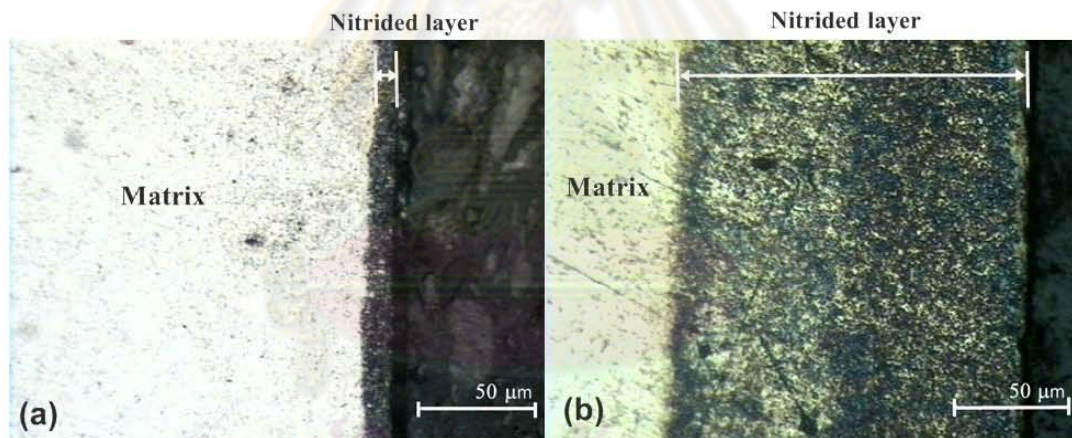


Figure 5.7: Cross-sectional H13 sample treated for 9 h (a), and 20 h (b) at 300 °C.

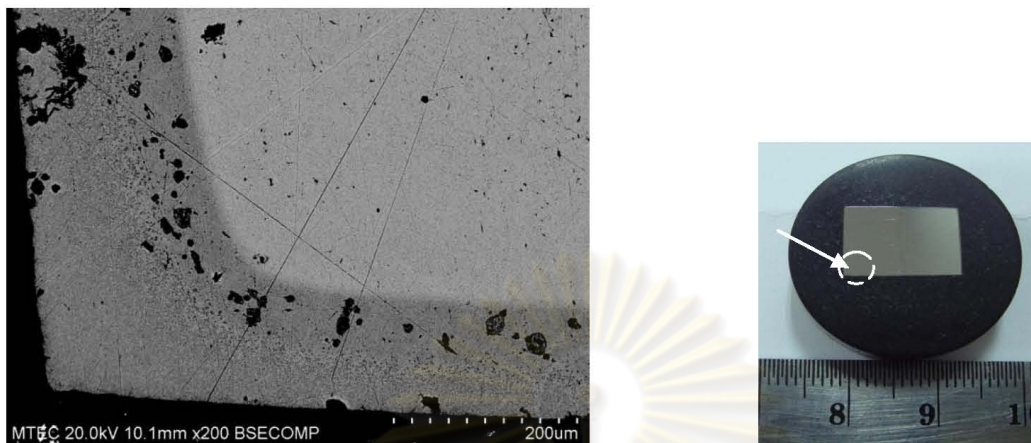


Figure 5.8: SEM micrograph showing the cross-section of edge of AISI H13 sample treated for 20 h.

EDX measurement was used to investigate the elemental composition after nitriding for 20 h, as shown in Fig.5.10. The elemental component including Fe, V, Cr, Si, C, O and N were detected. As we known, nitrogen is a light element which is difficult to detect by EDX because the low energy of the x-rays emitted from a sample, and then make a weakly signal for an energy dispersive spectrometer. However, nitrogen peak is shown all spectrums. This is probably due to the fact that the richer nitrogen participate spread over the nitride sample. Fig.5.10 shows the selected zone for investigation of the intensity of nitrogen peak. At zone A, and B present the small peak of nitrogen which cause the non-uniform of nitrogen participate.

ศูนย์วิจัยทรัพยากร
จุฬาลงกรณ์มหาวิทยาลัย

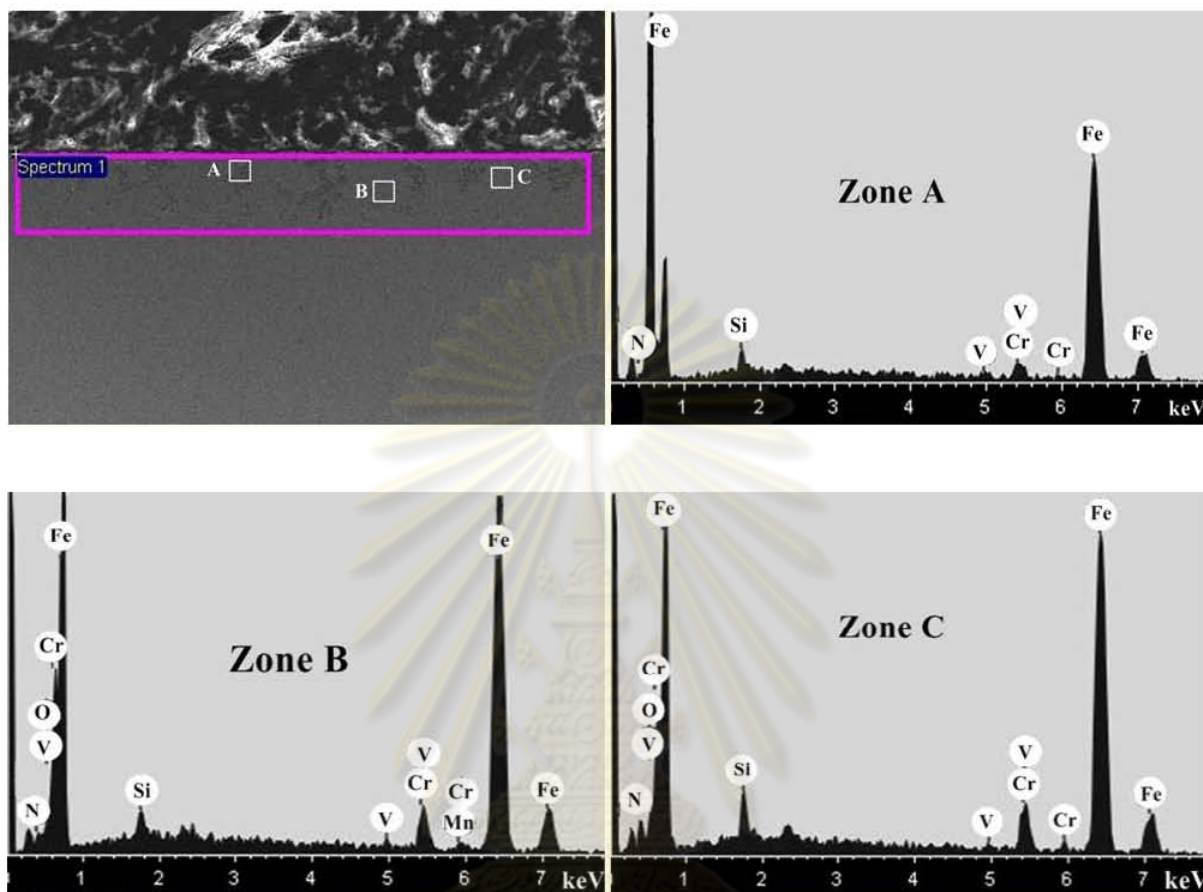


Figure 5.9: EDX composition profile of AISI H13 sample treated for 20 h.

To investigate of element distribution were obtained using EPMA mapping, as shown in Fig.5.10 and Fig.5.11, respectively. Fig.5.10 shows the concentration of nitrogen at the corner sample. The mapping shows the green color which means the relative high nitrogen participates in this area. Also, the cross-sectional of treated sample for 20 h (Fig.5.11) was mapped for indicating the element including Fe, N, and Cr. The clusters of light blue in nitrogen mapping represent the amount of nitrogen participate along depth profile of nitrides layer. On the map data, the red spot was shown in mapping of Cr which presents the high concentration of Cr participate. High Cr was detected maybe due to the remaining of Cr before plasma nitriding treatment or was

sputtered as nitriding process. Therefore, EPMA line scan was used to investigate the concentration along depth of nitrided sample, as shown in Fig.5.12 (b). On the line scan data, the atomic% of Fe, N, and Cr are not much different in nitrided layer zone at each depth from surface. But, we found that the Fe line scan at the matrix increase exponentially while Cr decreasing.

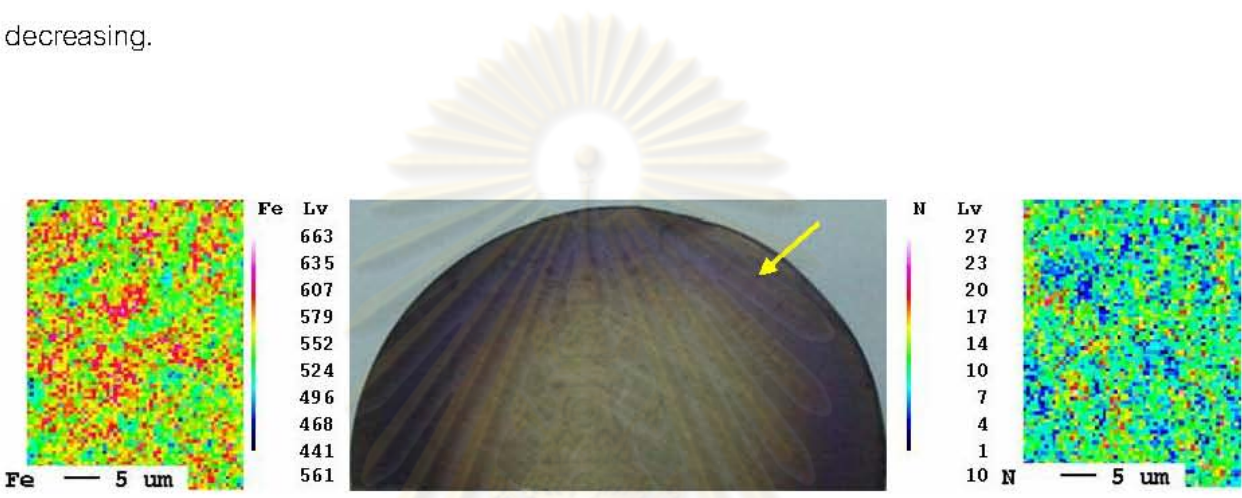


Figure 5.10: Electron probe microanalysis (EPMA) element maps (Fe, and N) of surface of the H13 treated at 20 h.

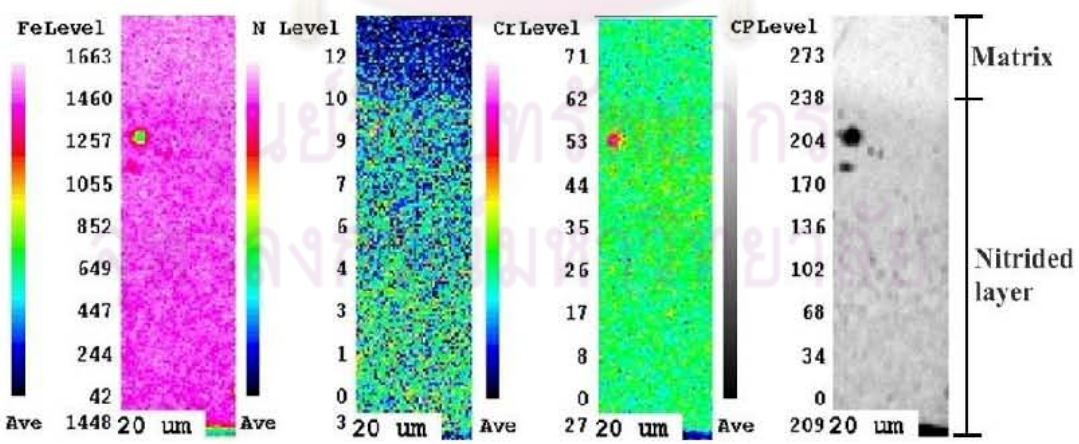


Figure 5.11: Electron probe microanalysis (EPMA) element maps (Fe, N, and Cr) of cross-sectional of the H13 treated at 20 h.

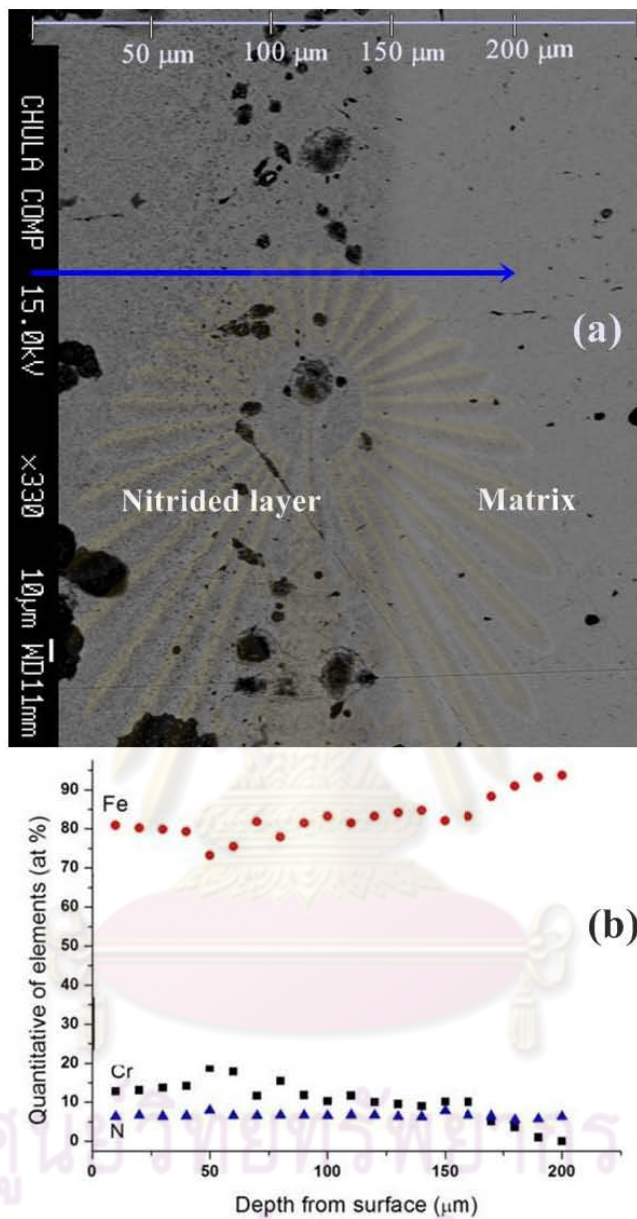


Figure 5.12: (a) Backscattered electron images showing the cross-section of nitrided H13 and (b) profiles of nitrogen, chromium, and iron concentration determined in the cross-section of nitrided H13 for 20 h.

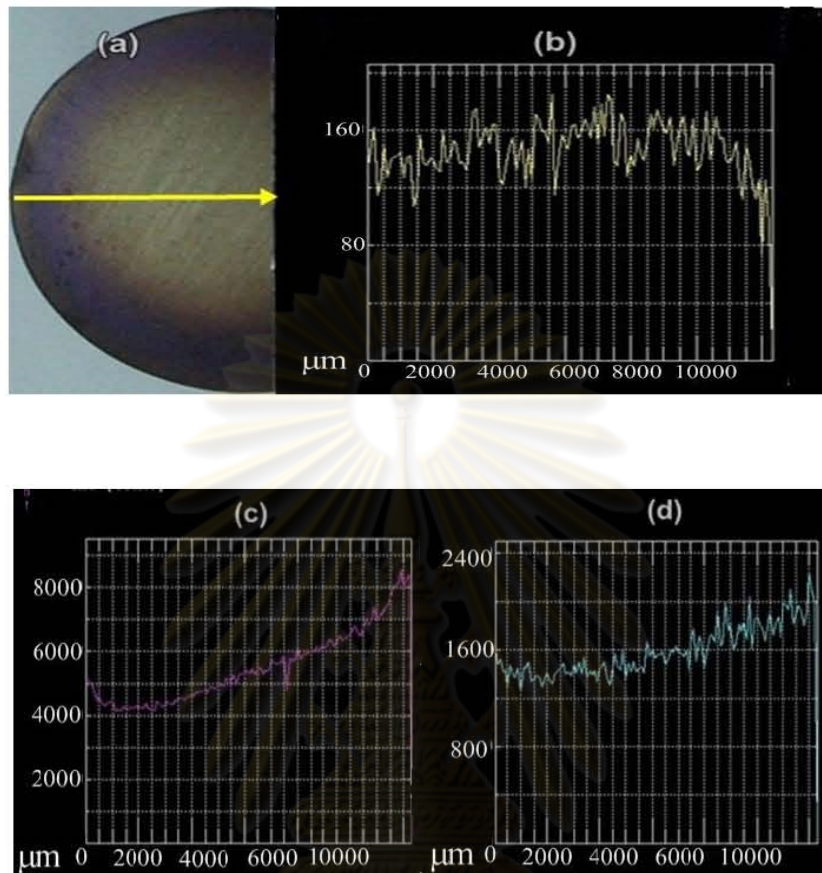


Fig. 5.13 Coloring of nitride sample (a) and compositional line scan of the h13 rf nitriding for 20 h; (b) nitrogen, (c) Iron; (d) Chromium

Similarly, we also investigated the compositional of element including Fe,N and Cr along surface of nitrided H13 sample, as given in Fig.5.13. From the scan image, the line is started in the sample from the edge to center in this case. It can be clearly seen in Fig.5.13 (a), that the color of the edge and center are different, which we can observe that the Fe concentration at the edge to be less than the center area. This is probably due to the fact that increasing time of nitriding process is caused the black color of the edge of nitride sample, which decreasing of Fe continuously towards the center of sample. The decreasing of Fe at the edge zone can be

concluded that irons are participated with another element. The sputter rate at the edge zone is higher than at the center zone of sample probably due to edge effect during nitriding process [95]. Moreover, along the EPMA scanning line is presented the higher chromium content in chromium nitride on the surface as scanning toward center of nitride sample.

The XRD patterns of nitride sample at different processing time (1h, 4h, 9h, 12h, and 20h) are shown in Fig. 5.14. After nitriding for 1 hour, only the diffraction peaks of α -Fe phase were observed at $2\theta = 44.7^\circ$, 65.0° , and 82.3° . With increasing nitriding time to 4 hours, low intensity peak of CrN can be detected. Basso et al. [19] was revealed the CrN for 4 h using DC plasma nitriding at temperature $> 440^\circ\text{C}$ while this work was detect CrN at 300°C . Due to the bombardment of high energy ions of rf discharge, the instantaneous temperature and short range penetration of ions into matrix could occur at the substrate surface [102]. GIXD profiles of the other samples with longer nitriding time than 4 hours show both CrN and γ -Fe₄N peaks indicates formation of both CrN and γ -Fe₄N phases in the nitrided layer. The presence of CrN peaks in GIXD profiles correspondences well with the microstructure and EPMA analysis that show precipitation of CrN particles. Considering the relative intensity of CrN ($2\theta=37.539$) and Fe₄N ($2\theta=47.969$) peaks comparing to Fe peaks, the relative intensity of both CrN and Fe₄N peaks becomes larger with increasing nitriding time. This indicates that the volume fraction of nitride precipitate particles and thickness of nitrided layer are increased with increasing nitriding time. The peaks shift and broadening might be due to the crystalline damage occurs due to bombardment of high energy ion and high density plasma which will be discussed in the next section.

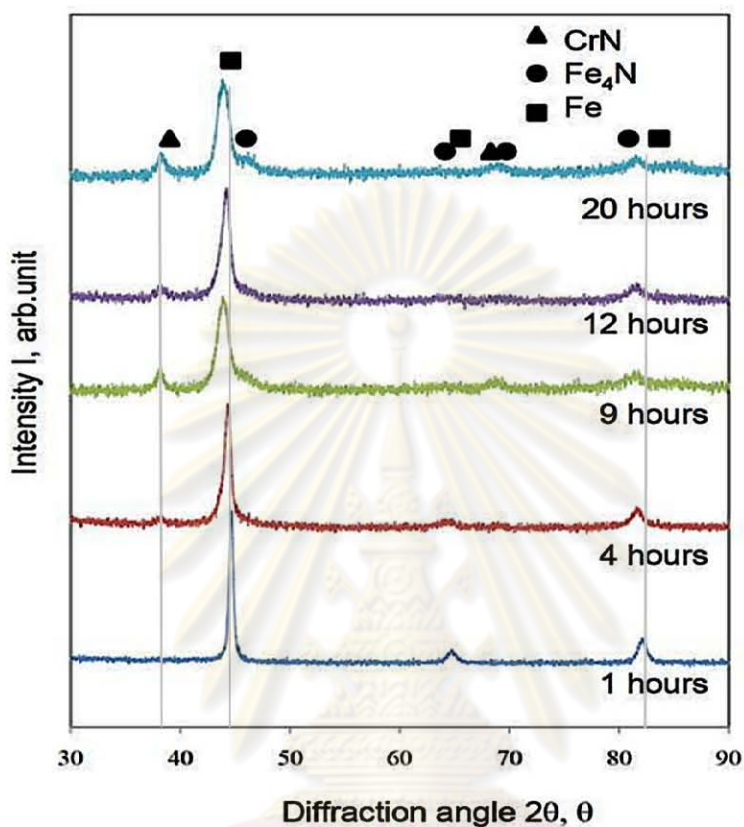


Figure 5.14: GIXD profiles at the incident angle of 3 degree of H13 sample after different nitriding time (1 to 20 hours).

From XRD result, the grain size was estimated using Scherrer equation which was used the full width at half-maximum (FWHM) from XRD peak of the bcc α -Fe (110) at different treatment time (1, 4, 9, 12, and 20 h). Broadening peak as prolonging treatment time was observed as shown in fig. 5.14. The grain size of bcc α -Fe (110) at $2\theta=44^\circ$ is decreased, corresponding to the increasing of broadening peak as longer treatment time. A smaller grain size approximately 8.42 nm for treatment time 20 h was calculated by Scherrer equation. As it is well known that peak broadening is caused by many reasons including crystallite size, instrument profile, microstrain, solid solution inhomogeneity, and temperature factor. In this case, the iron peak is

broad as increasing treatment time, implying that the grain size decreased as shown in Fig. 5.16.

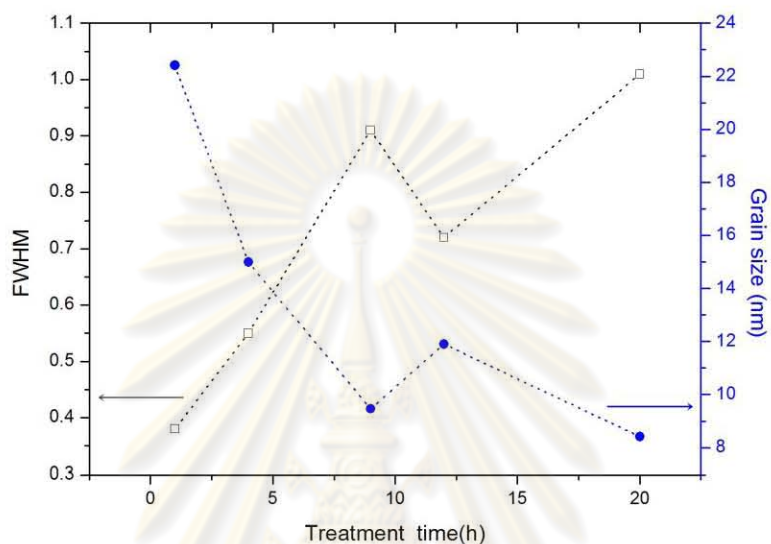


Figure 5.15: The FWHM of the XRD peak and the corresponding grain size of the broadening peak at $2\theta=44^\circ$ as a function of the treatment time (1, 4, 9, 12, and 20 h).

Surface hardness of all nitrided samples was obtained by Vicker's micro hardness with a load of 50 g as shown in Table 5.1. The surface hardness tends to increase with increasing nitriding time up to 9 hours. However, for nitriding time more than 9 hours, there is no significant change of surface hardness. From experiment results, we can conclude that the surface hardness of nitrided sample is significant increased after plasma nitriding for 9 hours and longer. Moreover, the surface hardness after plasma nitrided for 1 hour shows similar hardness with typical martensite which is a structure of H13 after heat treat and quenching. The hardness of 1 hour nitriding sample remains at same as as-quench sample due to short nitriding time that would not sufficient for the formation of nitride particles as indicated by GIXD profiles. According to the dependency of nitride precipitate particles on nitriding time, after 9 hours plasma nitriding significant amount of nitride particles were precipitate which results in

increasing of hardness up to 1072 HV. The improved hardness obtained by rf- ICP plasma nitriding is comparable to hardness achieved by typical DC plasma nitriding.

Table 5.1: Surface hardness of nitrided samples

| Nitriding Time (h) | Hardness(HV) 50g |
|--------------------|------------------|
| 1 | 631.70 |
| 4 | 796.26 |
| 9 | 1072.08 |
| 12 | 1048.86 |
| 20 | 1048.60 |

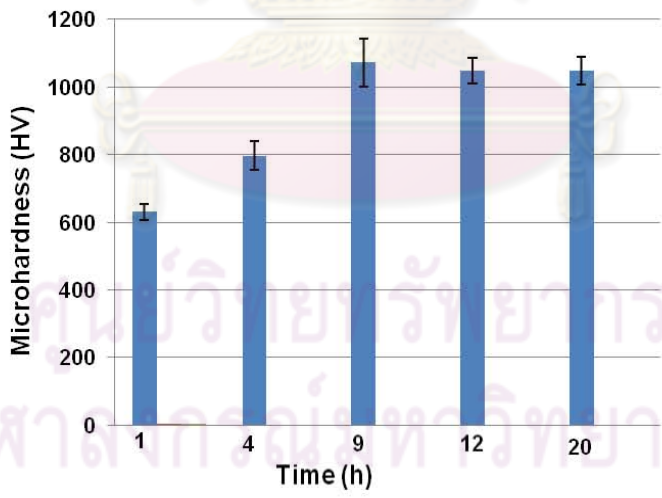


Fig.5.16: Variation of surface hardness with nitriding time

Nanomechanical, that is, Elastic modulus(E_r), Hardness (H), W_{elast} , W_{plast} , and W_{total} were also reported by nanoindentation with a Berkovich indenter. Table 5.2 shows the result of untreated and treated samples for 1 h, 9h, 12h, and 20h for the penetration depths of 200 nm. The hardness of nitride layer for 9 h is about 1825 HV greater than that of plasma nitriding for 20 h. However, the thickness of nitrided time for 20 h is still thick than treatment time for 9 h, as compared in Fig. 5.7. The elastic modulus of nitride layer for 9 h is about 255 GPa is also greater than that of nitride sample for 20 h. Kyung et al. [111] reported that the hardness-to-elastic modulus ratio (H/E_r) can be obtained the wear resistance of the film. Therefore, in the experiment result, the ratio of (H/E_r) at treatment time for 20 h shows higher than other conditions with can increase the wear resistance.

Table 5.2: E_r , H and W_{total} of nitrided sample

| sample | Elastic modulus [GPa] | Hardness (HV) | Hardness (Gpa) | W_{elast} (pJ) | W_{plast} (pJ) | W_{total} (pJ) |
|-----------|--------------------------|------------------|-------------------|---------------------|---------------------|---------------------|
| untreated | 211.00 | 608.00 | 6.50 | 112.80 | 299.70 | 412.60 |
| 1h | 245.60 | 925.40 | 9.50 | 187.00 | 453.00 | 641.00 |
| 9h | 255.00 | 1825.00 | 19.00 | 513.00 | 448.00 | 961.00 |
| 12h | 264.00 | 1291.00 | 13.90 | 323.00 | 496.00 | 820.00 |
| 20h | 191.00 | 1630.00 | 17.00 | 465.00 | 427.00 | 893.00 |

As we know during plasma nitriding process, the deposition process also happens, for investigate how much thick nitride has deposited on sample holder, therefore; the si wafer was placed on the substrate holder and closely with nitrided sample at treatment time for 20 h. The aim of this part is to investigate the composition of the deposited iron nitride layer as plasma nitriding process. Fig. 5.16(b) shows the surface of a Si substrate after plasma nitriding 20 h. Following the treatment, the coalescence of the deposited composite film was observed. EPMA

mapping (Fig.5.17) of the sample indicated that various element deposited on Si wafer during nitriding process including N, Si, Fe, Cr, O, V, and Al. Moreover, the resulting spectra of untreated and treated of Si wafer obtained from LIFH, LDE1, TAP, and PETJ crystals are shown in Fig.5.18 and 5.19, respectively. The results show the nitrogen atom deposited on si wafer which means during nitriding process nitrogen atom not only participate in sample by implant and thermal diffusion but also deposited on the treated sample.

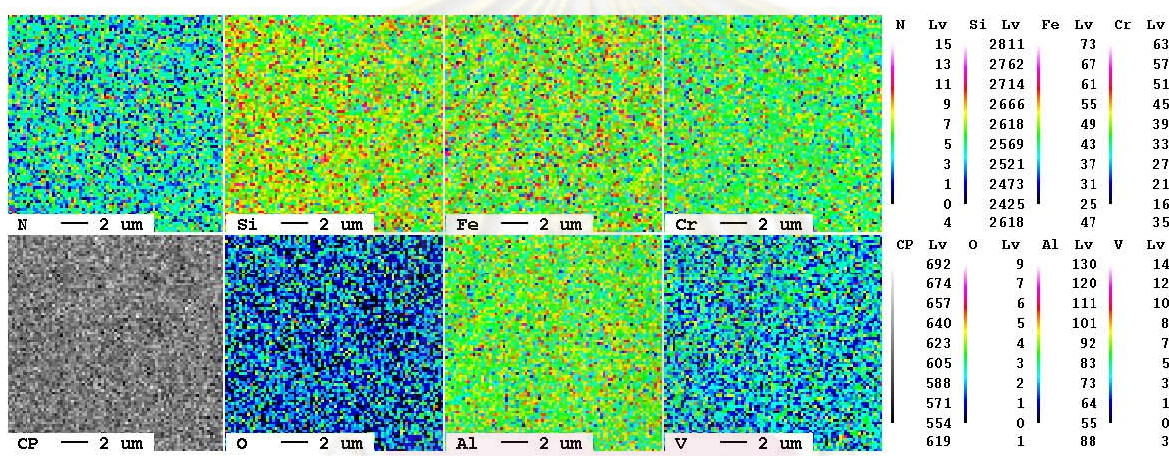


Figure 5.17: Element map showing the distribution of N, Si, Fe, Cr, O, V, and Al in a sample for treatment time 20 h.

At this condition, cross sectional was investigated by using SEM, as shown in Fig 5.20. Before testing, si wafer was cut by diamond pen for avoiding of thickness effect including cracking. By doing this, the thickness of approx. 260 nm was observed.

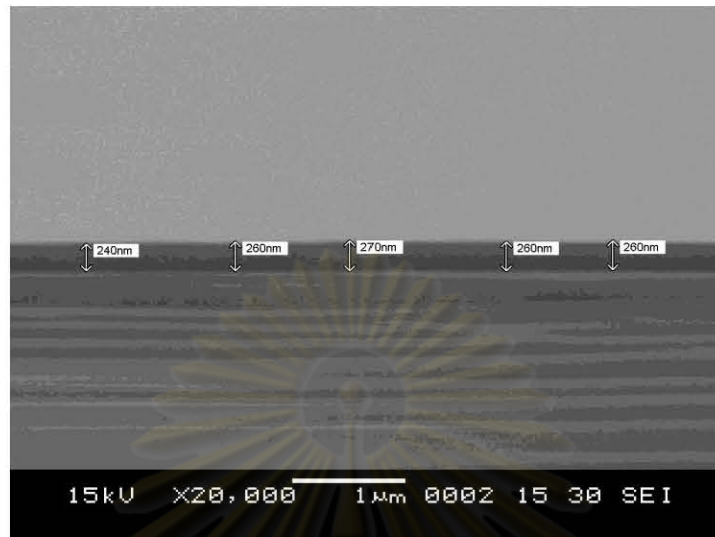


Figure 5.18: SEM micrograph of cross-section film deposited on silicon wafer during plasma nitriding AISI H13 for 20 h.

5.3.2 Summary

Low temperature with low RF power (100W) plasma nitriding can successfully form hard nitrided layer on the surface of H 13 tool steel. The surface hardness of AISI H13 tool steel treated by rf- ICP plasma nitriding significantly increases up to more than 1000 HV after nitriding for more than 9 hours. In this experiment, the nitrided layer could be formed at relatively low nitriding temperature (300°C) because of both pre-ionizing process by rf field and high amount of high energy ions which caused by the rf-ICP plasma generator. These effects leads to effective nitrogen transport on the atop sample surface and formation of nitrided layer. Moreover, the treatment time for 20 h can be formed the nitrided layer up to $150\ \mu\text{m}$, which was very short time compared to with Basso [19] et al. They report that AISI H13 were nitrided at nitriding time 36 h can achieve the thickness approx. $66.8\ \mu\text{m}$.

CHAPTER VI

CONCLUSIONS

In this work, the radio frequency inductively coupled plasma (rf-ICP) was used to form a nitrided layer on aluminium alloy and AISI H13 steel. The rf-ICP shows the advantage over the conventional plasma source (DC) including high density plasma. Moreover, it can be used at lower gas pressure and can be treated insulating material. To achieve the nitrided layer on aluminium alloy using dc plasma source is not easy because of the aluminium oxide. As referred by other researchers, they suggest that pre-sputtering is necessary. However, the thin nitrided layer was formed which is not significant to improve the mechanical properties of material. RF Plasma nitriding at a low pressure can be removed the oxygen remaining in the chamber. Therefore, rf plasma nitriding has been studied. The nitriding of Al2011 has been used to study at different treatment time. The XRD analysis confirmed the presence of a hexagonal AlN(100) on the substrate. The EPMA found the distribution of nitrogen spread the entire sample. All conditions show higher concentration of oxygen on the nitrided layer. Moreover, long treatment time (>25h) present the high surface roughness and thin nitride layer on aluminium surface. However, the rf plasma nitriding of Al2011 has not been successful because not achieve the thick nitrided layer though increasing treatment time up to 36 h. Afterwards, the sample was changed to Al-6wt%Cu for rf plasma nitriding at different the percentage composition in a gas mixture. The surface morphology and surface roughness are no significant difference between the nitriding of Al2011 and Al-6wt%Cu. Also, the hardness does not change much even though change the percentage of hydrogen in the nitriding gas mixture. Both of Al2011 and Al-6wt%Cu plasma nitriding has been found the white color on the sample cause a very high sputtering rate which increase the surface roughness. From the experimental results, we can conclude that the rf plasma nitriding cannot be used for aluminium alloy for improving the surface modification.

Thereafter, the AISI H13 was used in rf plasma nitriding with hydrogen-nitrogen gas mixture at working pressure 0.5 torr, and the substrate temperature of 300°C as different treatment time (1, 4, 9, 12 and 20 h). Hardness after a 4 h plasma nitriding time was found to be increased up to 796 HV and 925 HV using Vickers hardness testing, nanoindentation testing, respectively. In addition, the maximum hardness was observed after 9 h of treatment at 300°C. The nitrided H13 layers up to 150 µm in thickness have been formed with a nitriding time of 20 h. Therefore, the effect of nitriding time, in the range from 9 to 20 h, was significant.



ศูนย์วิทยทรัพยากร
จุฬาลงกรณ์มหาวิทยาลัย

References

- (1) Schoser, S., and others. XPS investigation of AlN formation in aluminium alloys using plasma source ion implantation. **Surface and Coatings Technology** 103-104 (May 1998): 222-226.
- (2) Castro, G., Fern´andez-Vicente, A., and Cid, J. Influence of the nitriding time in the wear behavior of an AISI H13 steel during a crankshaft forging process. **Wear** 263 (September 2007):1375-1385.
- (3) Salas, O., Oseguera, J., Garcia, N., and Figueroa, U. Nitriding of an H13 die steel in a dual plasma reactor. **Journal of Materials Engineering and Performance** 10 (December 2001): 649-655.
- (4) Moller, W., Parascandola, S., Telbizova, T., Gunzel, R., and Richter, E. Surface process and diffusion mechanisms of ion nitriding of stainless steel and aluminium. **Surface and Coatings Technology** 136 (February 2001): 73-79.
- (5) Zeghni, A.E., and Hashmi, M.S.J. The effect of coating and nitriding on the wear behavior of tool steels. **Journal of Materials Processing Technology** 155–156 (November 2004): 1918–1922.
- (6) Moradshahi, M., Tavakoli, T., Amiri, S., and Shayeganmehr, Sh. Plasma nitriding of Al alloys by DC glow discharge. **Surface and Coatings Technology** 201 (October 2006): 567-574.
- (7) Genel, K., and Demirkol, M. A method to predict effective case depth in ion nitride steels. **Surface and Coatings Technology** 195 (May 2005): 116-120.

- (8) Capa, M., Tamer, M., Gulmez, T., and Bodur, C.T. **Turkish Journal of Engineering & Environmental Science** 24 (2000): 111-117.
- (9) Gredelj, S., Gerson, A.R., Kumar, S., and Stewart McIntyre, N. Plasma nitriding and in situ characterization of aluminium. **Applied Surface Science** 199 (October 2002): 234-247.
- (10) Renevier, N., Czerwec, T., Billard, A., Stebut, J.von., and Michel, H. A way to decrease the nitriding temperature of aluminium: the low –pressure arc-assisted nitriding process. **Surface and Coatings Technology** 116-119 (September 1999): 380-385.
- (11) Schwabedissen, A., Benck, E.C., and Roberts, J.R. Langmuir probe measurements in an inductively coupled plasma source. **Physical Review E** 55 (March 1997): 3450-3458.
- (12) Vissutipitukul, V., Aizawa, T., and Kuwahara, H. Feasibility of plasma nitriding for effective surface treatment of pure aluminium. **Materials Transactions** 44 (May 2003):1412-1418.
- (13) Lee, Y.J., and Kang, S-W. Growth of aluminium nitride thin films prepared by plasma-enhanced atomic layer deposition. **Thin Solid Films** 446 (January 2004): 227-231.
- (14) Chen, H. Y., Stock, H. R., and Mayr, P. Plasma-assisted nitriding of aluminium. **Surface and Coatings Technology** 64 (June 1994): 139-147.
- (15) Gredelj, S., Gerson, A.R., Kumar, S., and Cavallaro, G.P. Characterization of aluminium surfaces with and without plasma nitriding by X-ray photoelectron spectroscopy. **Applied Surface Science** 174 (April 2001): 240-250.

- (16) Gredelj, S., Kumar, S., Gerson, A.R., and Cavallaro, G.P. Radio frequency plasma nitriding of aluminium at high power levels. *Thin Solid Films* 515 (December 2006): 1480-1485.
- (17) El-Hossary, F. M., Negm, N. Z., Khalil, S. M., and Raaif, M. Surface modification of titanium by radio frequency plasma nitriding. *Thin Solid Films* 497 (February 2006): 196-202.
- (18) Wen, D-C. Influence of layer microstructure on the corrosion behavior of plasma nitride cold work tool steel. *Journal of Materials Science* 45 (March 2010): 1540-1546.
- (19) Basso, R. L. O., and others. Microstructure and corrosion behavior of pulsed plasma-nitrided AISI H13 tool steel. *Corrosion Science* 52 (September 2010): 3133-3139.
- (20) Kim, S. K. , Yoo, J.S., Priest, J.M., and Fewell, M.P.Characteristics of martensitic stainless steel nitride in a low-pressure RF plasma. *Surface and Coatings Technology* 163-164(January 2003): 380-385.
- (21) Leite, M.V., Figueroa, C.A., Gallo, S. C., Rovani, A.C., and Basso, R.L.O. Wear mechanisms and microstructure of pulsed plasma nitride AISI H13 tool steel. *Wear*. 269 (July 2010): 466-472.
- (22) Cardarelli, F. *Materials Handbook*. 2nd ed. USA: Springer, 2008.
- (23) Hatch, J.E. *Properties and Physical Metallurgy*. USA: ASM International, 1984.
- (24) Kissell, J.R., and Ferry, R.L. *Aluminium Structures*. New York: John Wiley & Sons, 2002.
- (25) Wessel, J.K. *Handbook of advanced Materials*. USA: Willey-Interscience, 2004.

- (26) Polmear, L. **Light Alloys from Traditional Alloys to Nanocrystals**. 4th ed. UK: Elsevier oxford, 2006.
- (27) Visuttipitukul, T., and Aizawa, T. Plasma nitriding design for aluminium and aluminium alloys. **Surface Engineering** 22 (January 2006): 187-195.
- (28) Prbhudev, K.H. **Handbook of Heat Treatment of Steels**. New Delhi: Tata McGraw-Hill, 1988.
- (29) Kheirandish, S, and Noorian, A. Effect of Niobium on microstructure of cast AISI H13 Hot Work Tool Steel. **Journal of Iron and Steel Research** 15 (July 2008): 61-66.
- (30) Navinsek, B., and Seal, S. **Journal of the Minerals Metals & Materials Society** 53 (1997): 51-54.
- (31) Hochman, R. F. Effects of nitrogen in metal surfaces, **Proceedings of an International Conference on Ion Nitriding**, Ohio, USA, 1986, pp. 23-30.
- (32) Jin, H-Y., Wang, W., Gao, J-Q., Qiao, G-J., and Jin, Z-H. **Study of machinable AlN/BN ceramic composites**, *Material Letters* 60(2006): 190-193.
- (33) George E.T., and Maokenzie, D.S. **Handbook of aluminium**. USA: CRC Press, 2003.
- (34) Reier, T., Schultze, J.W., Osterle, W., Buchal, Chr. Nucleation and growth of AlN nanocrystallites prepared by N_2^+ implantation. **Surface and Coating Technology** 103-104 (May 1998): 415-420.
- (35) Mussler, B. H. **Advance Materila & Powders Handbook Alumminium nitride (AlN)**[Online]. Available from: <http://www.anceram.de> [2010, September 9].
- (36) Elangovan, T., Kuppusami, P., Thirumugesan, R., Ganesan, V., Mohandas, E., and Mangalaraj, D. Nanostructure CrN thin films prepared by reactive pulsed DC

- magnetron sputtering. **Materials Science and Engineering: B** 167 (February 2010): 17-25.
- (37) Weber, T., and others. Hardness and corrosion resistance of single-phase nitride and carbide on iron. **Materials Science and Engineering: A** 199 (August 1995): 205-210.
- (38) Li, Y., Wang, L., Zhang, D., Shen, L. The effect of surface nanocrystallization on plasma nitriding behavior of AISI 4140 steel. **Applied Surface Science** 257(August 2010): 979-984.
- (39) Tong, W.P., and others. Gaseous nitriding of iron with a nanostructured surface layer. **Scripta Materialia** 57(June 2007): 533-536.
- (40) Navi Granito. Surface material design and control in steels for automotive parts by plasma nitriding technique. **Doctoral dissertation**, Faculty of engineering The University of Tokyo, 2003.
- (41) Lampman, S. **Heat Treatment: Introduction to surface Hardening of Steel**. 2 vols. ASM International, 1991.
- (42) Figueroa, U., Salas, O., and Oseguera, J. Production of AlN films: ion nitriding versus PVD coating. **Thin solid films** 469-470(October 2004): 295-303.
- (43) Tucker, R.C. **ASM Handbook: Surface Engineering: Thermal Spray Coating** 5 vols. ASM International, 1994.
- (44) Taylor, M-A., Hulett, D.M. A comparison between ion nitriding and ion implantation. **Proceeding of an International conference on ion nitriding**. (1986) 199-203.
- (45) Sonnleitner, M., Spiradek-Hahm, K., Rossi, F. Microstructure of plasma nitride layers on aluminium. **Surface and Coating Technology** 156 (2002): 149-154.

- (46) Blawert, C., Mordike, Plasma immersion ion implantation of pure aluminium at elevated temperatures. **Nuclear Instruments and Methods in Physics Research B** 127-128 (1997): 873-878.
- (47) Peng, W-Y, Wu, X-C, Min, Y-A, and Xu, L-P. Effect of the compound layer of plasma nitriding on thermal fatigue behavior of 4 Cr5MoSiV1 die steel, **Journal of Shanghai University** 7 (2003): 87-92.
- (48) Davis, J. R. **Wrought High-Speed Tool Steels**. USA: ASM International, 1995.
- (49) Rolinski, E., and Sharp, G. The effect of sputtering on kinetics of compound zone formation in the plasma nitriding of 3% Cr-Mo-V steel. **Journal of Materials Engineering and Performance** 10 (March 2001): 444-448.
- (50) Rakhit, A.K. **Heat treatment of gears: a practical guide for engineers**. USA: ASM International, 2000.
- (51) Flake C. Campbell, **Elements of metallurgy and engineering alloys**. USA: ASM International, 2008.
- (52) Baranowska, J., and Wysiecki, M. Influence of surface pretreatment on case formation during gaseous nitriding. **Surface and Coating Technology** 125 (March 2000): 30-34.
- (53) Hoyle, G. **High Speed Steels**. England: Butterworth, 1988.
- (54) Paul Murray Bellan, **Fundamentals of plasma physics**, Cambridge University Press, 2006.
- (55) Plasma applications, Proceeding of the Regional College on plasma Applications
- (56) Alexander A. F., and Lawrence A. K. **Plasma physics and engineering**, New York: Taylor & Francis, 2004.

- (57) Samant, C. C., Rupji, A. D., Gogawale, S.V., Kothari, D.C., and Kulkarni, V.H. Study of surface hardness of Al-6063 under plasma nitridation. **Surface and Coating Technology** 158-159 (September 2002): 658-663.
- (58) Mahboubi, F., Abdolvahabi. K. The effect of temperature on plasma nitriding behavior of DIN 1.6959 low alloy steel. **Vacuum** 81(October 2006): 239-243.
- (59) Gredelj, S. **Plasma nitriding of 2011 aluminium alloy**. Doctoral dissertation, Ian Wark Research Institute, ARC Special Research Centre University of South Australia, 2002.
- (60) Korhonen, A.S., Harju, E. Advance in vacuum metallurgy effects on the heat treatment and surface engineering of metals. 20 th ASM Heat treatment society conference Proceeding,USA, 2000, pp. 284-289.
- (61) Michel, H., Czerwiec. T., Gantois. M., Ablitzer. D., and Ricard. A. Progress in the analysis of the mechanisms of ion nitriding. **Surface and Coating Technology** 72 (May 1995): 103-111.
- (62) Paul Hubbard. Characterisation of a commercial Active Screen Plasma Nitriding System. **Doctoral dissertation**, Department of Applied Physics Faculty of science RMIT University, 2007.
- (63) Ensinger, W. Modification of mechanical and chemical surface properties of metals by plasma immersion ion implantation. **Surface and Coating Technology** 100-101(1998): 341-352.
- (64) Paul, K.C., and Sakuta, T., Properties study of inductively coupled nitrogen plasmas and pressure effects on them. **Electric Power Systems Research** 56(December 2000): 185-193.

- (65) Liang, W. Surface modification of AISI 304 austenitic steel by plasma nitriding. **Applied Surface Science** 211(April 2003): 308-314.
- (66) Moradshahi, M., Tavakoli, T., Amiri, S., and Shayeganmehr, Sh. Plasma nitriding of Al alloys by DC glow discharge. **Surface and Coating Technology** 201(October 2006): 567-574.
- (67) Cruz, M.R., Nachez, L., Gomez, B.J., Nosei, L. Feugeas, J.N., and Staia, M.H. Ion nitride AISI H13 tool steel Part I- Microstructural aspects. **Surface Engineering** 22(2006): 359-366.
- (68) Rodrigo L.O. and others, Microstructure and corrosion behavior of pulsed plasma-nitrided AISI H13 tool steel. **Corrosion Science** 52(June 2010): 3133-3139.
- (69) Visuttipitukul, P., Paa-rai, C., and Kuwahara, H. Characterization of plasma nitrided AISI H13 tool steel. **Acta Metallurgica Slovaca** 12(2006): 264-274.
- (70) Sugawara, Plasma etching UK:Oxford science publication 1998
- (71) University of Malaya. **Literature review** [online]. Available from: <http://dspace.fsktm.um.edu.my/bitstream/1812/490/2/chapter%201.pdf> [2011, January 28]
- (72) Czerwiec, T. Greer, F., and Graves, D. B. **Journal Applied Physics** 38 (2005): 4278-4289.
- (73) Winchester, M.R., and Payling, R. Radio-frequency glow discharge spectrometry: A critical review. **Spectrochimica Acta Part B** 59(February 2004): 607-666.
- (74) Gredelj, S., Gerson, A. R., Kumar, S., and Cavallaro, G. P. Inductively coupled plasma nitriding of aluminium. **Applied Surface Science** 199 (October 2002): 183-194.

- (75) Valencia-Alvarado, R., and others. Nitriding of AISI 304 stainless steel in a 85% H₂/15% N₂ mixture with an inductively coupled plasma source. **Vacuum** 82 (2008): 1360-1363.
- (76) A. B. M. S Azam, Abd. H. Hamidon and S. Xu. **Vacuum** 73 (2004): 487-492
- (77) Baldwin, M.J., and others. RF-plasma nitriding of stainless steel. **Surface and Coatings Technology** 98 (January 1998): 1187-1191.
- (78) Renevier, N., Czerwicz, T., Collignon, P., and Michel, H. Diagnostic of arc discharges for plasma nitriding by optical emission spectroscopy. **Surface and Coating Technology** 98 (January 1998): 1400-1405.
- (79) Negm, N.Z. A study of rf plasma nitriding at constant power in different H₂-N₂ mixtures at different temperatures. **Materials Science and Engineering: B** 129 (April 2006): 207-210.
- (80) Marchand, J.L., Michel, H., Gantois, M. Emission spectroscopy of N₂-H₂ D.C. discharge for metal surface nitriding. Proceeding of an International conference on ion nitriding. (1986) 53-57.
- (81) Figueroa, C.A., and Alvarez, F. On the hydrogen etching mechanism in plasma nitriding of metals. **Applied Surface Science** 253 (April 2006): 1806-1809.
- (82) Ceylan, A., Kaynak, E., Ozcan, S., and Firat, T. **Turkish Journal of Physics** 28 (2004): 265-269.
- (83) Czerwicz, T., Renevier, N., and Michel, H. Low-temperature plasma-assisted nitriding. **Surface and Coating Technology** 131 (2000): 267-277.

- (84) Granito, N., Kuwahara, H., Aizawa, T., Graded hardness design in the surface modified steels by plasma nitriding, 20 th ASM Heat treatment society conference Proceeding,USA, 2000, pp.227-232
- (85) Ul-Hamid, A., Tawancy, H-M., Mohammed, A-R I., Al-Jaroudi, S-S., and Abbas, N-M. Quantitative WDS analysis using electron probe microanalyzer. **Material Characterization** 56 (2006): 192-199.
- (86) Mori, D., Yamada, K. A review of recent application of EPMA to evaluate the durability of concrete. **Journal of advanced concrete technology** 5 (October 2007): 285-298
- (87) Thormann, E., Pettersson, T., Kettle, J., and Claesson, P.M. **Ultramicroscopy** 110 (2010): 313-319.
- (88) [Online]. Available from: <http://web.iyte.edu.tr/~sedatakkurt/me409/om.pdf>[2010, September]
- (89) Brandon, D., and Kaplan, W-D. **Microstructural Characterization of Materials**. USA : John Wiley & Sons, 2001.
- (90) **Vicker hardness testing** [Online]. Available from: <http://www.matweb.com/reference/vickers-hardness.aspx>[2010, October]
- (91) Lee, K-H., and Takai, O. **Diamond & Related Materials** 14(February 2005):1444-1450.
- (92) Pergande, S. R., Polycarpou, A.A., and Conry, T.F. Use of Nano-Indentation and Nano-Scratch Technique to investigate Near Surface Material Properties. **Associated With Scuffing of Engineering Surface**. University of Illinois at Urbana –Champaign

- (93) Jian, S-R., Chen, G-J., and Lin, T-C. Berkovich Nanoindentation on AlN Thin Films. **Nanoscale Research Letters** 5 (March 2010): 935-940.
- (94) Alves Jr, C., de Araujo, F.O., Ribeiro, K.J.B., da Costa, J.A.P., Sousa, R.R.M., Sousa, R.S. Use of cathodic cage in plasma nitriding. **Surface and Coating Technology** 201 (June 2006): 2460-2454.
- (95) Olzon-Dionysio, M., Campos, M., Kapp, M., Souza, S., de Souza, S.D. Influences of plasma nitriding edge effect on properties of 316L stainless steel. **Surface and Coating Technology** 204 (April 2010): 3623-3628.
- (96) Taweesub, K., Visutti pitukul, P., Tungkasmita, S., and Paosawatanyong, B. **Surface and Coatings Technology** 204 (2010): 3091-3095.
- (97) Ouyang, L.H., Rode, D.L., Zulkifli, T., and Abraham-Shrauner, B. Hydrogenated amorphous and microcrystalline GaAs films prepared by radio-frequency magnetron sputtering. **Journal of Applied Physics** 91(March 2002): 3459-3467.
- (98) P. Hubbard, S.J. Dowey, J.G. Partridge, E.D. Doyle and D.G. McCulloch: **Surface Coating Technology** 204(2010): 1151-1157.
- (99) Samardzija, Z., Makovec, D., and Ceh, Miran, EPMA and Microstructural Characterization of Yttrium Doped BaTiO₃. **Ceramics. Mikrochimica Acta** 132(2000): 383-386.
- (100) Jian, S-R., Chen, G-J., and Lin, T-C. Berkovich Nanoindentation on AlN Thin Films. **Nanoscale Research Letters** 5 (March 2010): 935-940.
- (101) Ahangarani, Sh, Mahboubi, F., Sabour, and A.R. Effects of various nitriding parameters on active seen plasma nitriding behavior of a low-alloy steel. **Vacuum** 80(2006): 1032-1037.
- (102) C.S. Moon, J.G. Han, **Thin solid films** 516 (2008): 6560-6564.



APPENDIX

ศูนย์วิทยทรัพยากร
จุฬาลงกรณ์มหาวิทยาลัย

Appendix A

Conference presentations and publications

International Presentation

2010. J. Pongsopa, B. Paosawatyanong, P. Visuttpitukul. Surface hardening of aluminium-copper alloy 2011 by rf plasma nitriding process. Oral presentation at 8th International Conference on Fracture & Strength of Solids 2010, the Istana Hotel, Kuala Lumpur, Malaysia, (7-9 June; 2010).

2010. J. Pongsopa, B. Paosawatyanong, P. Visuttpitukul. Effect of hydrogen in rf plasma nitriding on aluminium alloy. Poster presentation at The International Symposium on Advanced Plasma Science and its Applications for Nitrides and Nanomaterials [Isplasma2010], Meijo University, Nagoya, Japan, (7-10 March; 2010)

2009. J. Pongsopa, B. Paosawatyanong, P. Visuttpitukul. RF Plasma nitriding of aluminium copper alloy. Oral presentation at International Conference on Plasma Surface Engineering (AEPSE2009), Busan, South Korea, (20-25 September; 2009).

Publication:

2011. J. Pongsopa, B. Paosawatyanyong, P. Visuttpitukul. Surface Hardening of aluminium – copper alloy 2011 by rf plasma nitriding process. *Key Engineering Materials*, Volume 462-263, pages 1097-1102. (2011).

2011. J. Pongsopa, P. Visuttpitukul, B. Paosawatyanyong. Effect of hydrogen in rf plasma nitriding on Al-6wt%Cu alloy. *Applied Mechanics and Materials*, Volume 55-57, pages 1063 - 1066. (2011).



ศูนย์วิจัยทรัพยากร
จุฬาลงกรณ์มหาวิทยาลัย

Appendix B

JCPD of AlN

| Pattern : 00-025-1133 | | Radiation = 1.540598 | | Quality : High | | |
|--|---------------------|--------------------------------|----------|----------------|----------|----------|
| AlN | | 2 θ | <i>l</i> | <i>h</i> | <i>k</i> | <i>j</i> |
| Aluminum Nitride | | 33.216 | 100 | 1 | 0 | 0 |
| | | 36.041 | 60 | 0 | 0 | 2 |
| | | 37.917 | 80 | 1 | 0 | 1 |
| | | 49.816 | 25 | 1 | 0 | 2 |
| | | 59.350 | 40 | 1 | 1 | 0 |
| | | 66.054 | 30 | 1 | 0 | 3 |
| | | 69.731 | 5 | 2 | 0 | 0 |
| | | 71.440 | 25 | 1 | 1 | 1 |
| | | 72.629 | 10 | 2 | 0 | 1 |
| | | 76.445 | 1 | 0 | 0 | 4 |
| | | 81.089 | 4 | 2 | 0 | 2 |
| | | 85.941 | 1 | 1 | 0 | 4 |
| | | 94.843 | 9 | 2 | 0 | 3 |
| | | 98.292 | 3 | 2 | 1 | 0 |
| | | 101.067 | 7 | 2 | 1 | 1 |
| | | 104.837 | 2 | 1 | 1 | 4 |
| | | 109.630 | 3 | 2 | 2 | 2 |
| | | 111.123 | 6 | 1 | 1 | 5 |
| | | 114.830 | 1 | 2 | 0 | 4 |
| | | 118.097 | 4 | 3 | 0 | 0 |
| | | 125.107 | 10 | 2 | 1 | 3 |
| | | 131.514 | 5 | 3 | 0 | 2 |
| | | 136.341 | 1 | 0 | 0 | 6 |
| | | 148.271 | 5 | 2 | 0 | 0 |
| | | 152.456 | 1 | 1 | 0 | 6 |
| | | 155.531 | 1 | 2 | 1 | 4 |
| Lattice : Hexagonal | Mol. weight = 40.99 | | | | | |
| S.G. : P63mc (186) | Volume [CD] = 41.74 | | | | | |
| a = 3.11140 | Dx = 3.261 | | | | | |
| c = 4.97920 | Meor = 1.60 | | | | | |
| Z = 2 | | | | | | |
| <p>Optical data: A-2.13, B-2.20, Sign-- Color: Light gray Temperature of data collection: Pattern taken at 25 C. Sample source or locality: Sample from Cerac/Pure, Inc. Menomee Falls, Wisconsin, USA. General comments: A small amount of metallic aluminum was sieved out. General comments: Major impurities: 0.01-0.1% each Fe, Mg, Si, 0.003-0.03% each Co, Cr, Cu, Sr, Ti, 0.001-0.01% each Ca, Ni. General comments: Merck Index, 8th Ed., p. 45. Additional pattern: To replace 00-008-0262. Data collection flag: Ambient.</p> | | | | | | |
| <p>Kohn et al., Am. Mineral., volume 41, page 355 (1956) Natl. Bur. Stand. (U.S.) Monogr. 25, volume 12, page 5 (1975) CAS Number: 24304-00-5</p> | | | | | | |
| Radiation : CuK α | | Filter : Monochromator crystal | | | | |
| Lambda : 1.54060 | | d-sp : Not given | | | | |
| SS/FOM : F26- 78(0.0119,28) | | Internal standard : W | | | | |

Vitae

Ms. Jiraporn Pongsopa was born on December 9th 1978 in Chaiyaphum, Thailand. I graduate bachelor's degree from Kasetsart University in Science-Physics Teaching, Thailand in April 1999. I completed my master degree in Science-Physics from Srinakarinwirot University in March, 2003.

After receiving bachelor's degree, I became a lecturer at Suandusit University for 1 year before have started in master degree for 3 year. After finished master degree, I backed to work at Suandusit University again for 1 year. After that, in June 2006, I started to study in Ph.D. degree of Nanoscience and Technology Program at Chulalongkorn University. My thesis focused on rf-ICP plasma nitriding of aluminium alloys and AISI H13.



ศูนย์วิจัยทรัพยากร
จุฬาลงกรณ์มหาวิทยาลัย